iScience

CellPress
OPEN ACCESS

Article

Potential anti-COVID-19 agents, cepharanthine and nelfinavir, and their usage for combination treatment

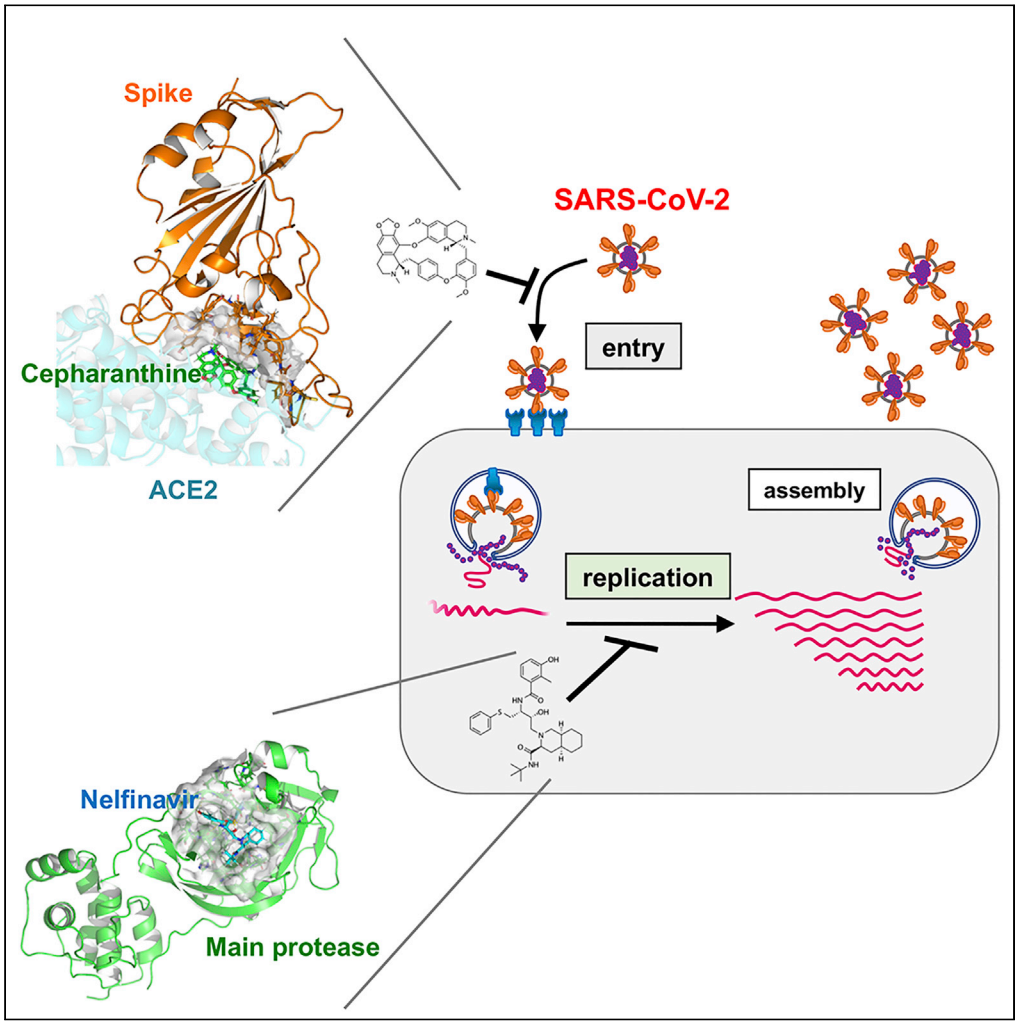

Hirofumi Ohashi, Koichi Watashi, Wakana Saso, ..., Makoto Takeda, Jane A. McKeating, Takaji Wakita

kwatashi@nih.go.jp

Highlights

Nelfinavir (NFV) inhibits SARS-CoV-2 replication

Cepharanthine (CEP) inhibits SARS-CoV-2 attachment to target cells

Combination of NFV and CEP can synergistically augment antiviral activity

NFV and CEP are estimated to shorten the time to viral elimination at clinical doses

Ohashi et al., iScience 24, 102367
April 23, 2021
https://doi.org/10.1016/j.isci.2021.102367

iScience

CellPress
OPEN ACCESS

Article

Potential anti-COVID-19 agents, cepharanthine and nelfinavir, and their usage for combination treatment

Hirofumi Ohashi,[1,2,30] Koichi Watashi,[1,2,3,4,29,30,31,*] Wakana Saso,[1,5,6,30] Kaho Shionoya,[1,2] Shoya Iwanami,[7] Takatsugu Hirokawa,[8,9,10] Tsuyoshi Shirai,[11] Shigehiko Kanaya,[12] Yusuke Ito,[7] Kwang Su Kim,[7] Takao Nomura,[13] Tateki Suzuki,[14] Kazane Nishioka,[1,2] Shuji Ando,[15] Keisuke Ejima,[16] Yoshiki Koizumi,[17] Tomohiro Tanaka,[18] Shin Aoki,[18,19] Kouji Kuramochi,[2] Tadaki Suzuki,[20] Takao Hashiguchi,[14] Katsumi Maenaka,[13,21,22] Tetsuro Matano,[5,6] Masamichi Muramatsu,[1] Masayuki Saijo,[15] Kazuyuki Aihara,[23] Shingo Iwami,[4,7,24,25,26] Makoto Takeda,[27] Jane A. McKeating,[28] and Takaji Wakita[1]

SUMMARY

Antiviral treatments targeting the coronavirus disease 2019 are urgently required. We screened a panel of already approved drugs in a cell culture model of severe acute respiratory syndrome coronavirus 2 (SARS-CoV-2) and identified two new agents having higher antiviral potentials than the drug candidates such as remdesivir and chroloquine in VeroE6/TMPRSS2 cells: the anti-inflammatory drug cepharanthine and human immunodeficiency virus protease inhibitor nelfinavir. Cepharanthine inhibited SARS-CoV-2 entry through the blocking of viral binding to target cells, while nelfinavir suppressed viral replication partly by protease inhibition. Consistent with their different modes of action, synergistic effect of this combined treatment to limit SARS-CoV-2 proliferation was highlighted. Mathematical modeling *in vitro* antiviral activity coupled with the calculated total drug concentrations in the lung predicts that nelfinavir will shorten the period until viral clearance by 4.9 days and the combining cepharanthine/nelfinavir enhanced their predicted efficacy. These results warrant further evaluation of the potential anti-SARS-CoV-2 activity of cepharanthine and nelfinavir.

INTRODUCTION

The novel coronavirus disease 2019 (COVID-19), caused by the infection of severe acute respiratory syndrome coronavirus 2 (SARS-CoV-2), is a global public health problem that is impacting social and economic damage worldwide (Huang et al., 2020; Zhou et al., 2020; Zhu et al., 2020). More than 5,000,000 confirmed cases with over 300,000 deaths were reported late May 2020 across 216 countries/areas/territories (WHO, 2020). COVID-19 was characterized as a pandemic by the World Health Organization (WHO), and new treatments along with a vaccine are urgently needed. Remdesivir (RDV), a nucleoside analog originally developed for treating Ebola virus along with several other Food and Drug Administration (FDA)-approved drugs, is being evaluated in patients with COVID-19: including lopinavir (LPV) boosted by ritonavir, chloroquine (CLQ), favipiravir (FPV), and interferon (Beigel et al., 2020; Boulware et al., 2020; Cao et al., 2020; Dong et al., 2020; Touret and de Lamballerie, 2020). Reports on the clinical efficacies of these drugs are pending; however, it would be prudent to have a pipeline of additional drug candidates available for clinical trials.

In this study, we screened a panel of already approved drugs in a SARS-CoV-2 infection cell culture assay and identified two, cepharanthine (CEP) and nelfinavir (NFV), that showed more potent antiviral activity compared to RDV and other drugs currently being trialed. Our *in vitro*, *in silico*, and cell culture analyses demonstrate that CEP and NFV inhibit SARS-CoV-2 entry and RNA replication, respectively. Their different modes of action provided synergistic antiviral effects. We also mathematically predicted the potential antiviral efficacy of the single treatment of either CEP or NFV and its combination in clinical settings. These data cumulatively provide evidence for anti-SARS-CoV-2 potentials of CEP and NFV.

[1]Department of Virology II, National Institute of Infectious Diseases, Tokyo 162-8640, Japan

[2]Department of Applied Biological Science, Tokyo University of Science, Noda 278-8510, Japan

[3]Institute for Frontier Life and Medical Sciences, Kyoto University, Kyoto 606-8507, Japan

[4]MIRAI, JST, Saitama 332-0012, Japan

[5]The Institute of Medical Science, The University of Tokyo, Tokyo 108-8639, Japan

[6]AIDS Research Center, National Institute of Infectious Diseases, Tokyo 162-8640, Japan

[7]Department of Biology, Faculty of Sciences, Kyushu University, Fukuoka 812-8581, Japan

[8]Cellular and Molecular Biotechnology Research Institute, National Institute of Advanced Industrial Science and Technology, Tokyo 135-0064, Japan

[9]Division of Biomedical Science, Faculty of Medicine, University of Tsukuba, Tsukuba 305-8575, Japan

[10]Transborder Medical Research Center, University of Tsukuba, Tsukuba 305-8575, Japan

[11]Faculty of Bioscience, Nagahama Institute of Bio-Science and Technology, Nagahama 526-0829, Japan

[12]Graduate School of Science and Technology, Nara Institute of Science and Technology, Ikoma 630-0192, Japan

Continued

RESULTS

Cepharanthine and nelfinavir inhibit SARS-CoV-2 infection

We established a cell-based drug screening system to identify compounds that protect cells from SARS-CoV-2-induced cytopathology (Figure 1A): VeroE6/TMPRSS2 cells were treated with compounds for 1 hr during inoculation with a clinical isolate of SARS-CoV-2 (Matsuyama et al., 2020) at a multiplicity of infection (MOI) of 0.01 (or 0.001 for the indicated assay). Unbound virus was removed by washing, and the cells were treated with compounds for 48 hr to assess cell viability (Figure 1A) (methods). SARS-CoV-2 replication in VeroE6/TMPRSS2 induced a cytopathic effect and to validate our assay we show that two compounds, LPV and CLQ, that were reported to inhibit SARS-CoV-2 infection (Choy et al., 2020; Pizzorno et al., 2020; Wang et al., 2020a) reduced virus-induced cytopathicity (Figure 1B, compare b and c, d). After screening 306 FDA/European Medicines Agency/Pharmaceuticals and Medical Devices Agency-approved drugs, we identified compounds that protected cell viability by 20-fold compared with a dimethyl sulfoxide solvent control (methods). Among these, we selected to study CEP and NFV as candidates showing the greatest anti-cytopathic activity (Figures 1B–g, h). CEP is a Stephania-derived alkaloid extract with anti-inflammatory and anti-oxidative activities, and NFV targets human immunodeficiency virus protease (Bailly, 2019; Kao et al., 2015; Markowitz et al., 1998). To confirm and extend these observations, we assessed SARS-CoV-2-encoded N protein expression 24 hr after inoculation by immunofluorescence (Figure 1C, red) and immunoblotting (Figure 1D). Both CEP and NFV significantly reduced N protein expression along with the positive control drug candidates LPV, CLQ, and RDV. We confirmed that CEP and NFV inhibit SARS-CoV-2 proliferation in a human-derived lung epithelial cell line Calu-3 cells (Figure 1E).

Dose-response curve for the anti-SARS-CoV-2 activity of cepharanthine and nelfinavir

To extend these observations, we quantified the effect of these compounds on secreted viral RNA and cell viability at 24 hr after infection. CEP and NFV significantly reduced viral RNA levels in a dose-dependent manner to 0.001–0.01% of the untreated control infections (Figure 2A). As expected, the positive control compounds (CLQ, LPV, and RDV) inhibited viral RNA, whereas FPV up to 64 μM showed negligible antiviral activity, consistent with previous reports (Choy et al., 2020; Jeon et al., 2020; Wang et al., 2020a). In parallel, we also assessed cell viability and noted cell death at high drug concentrations up to 64 μM (Figure 2B). The concentrations of drugs required to inhibit 50% (IC_{50}) or 90% (IC_{90}) of virus proliferation along with their 50% cytotoxicity (CC_{50}) were estimated by median effect model and are listed in Figures 2A and 2B. These experiments highlight a >70-fold window (CC_{50}/IC_{50}) where CEP and NFV can inhibit SARS-CoV-2 proliferation with minimal toxicity. In summary, our screen identified two compounds that inhibit SARS-CoV-2 infection with high potency.

Cepharanthine and nelfinavir have different modes of action

To determine how these compounds impact on the viral replicative life cycle, we performed a time-of-addition assay (Figure 3A). We measured the antiviral activity of drugs added at different times: (a) present during the 1 hr virus inoculation step and maintained throughout the 24 hr infection period ("whole life cycle"); (b) present during the 1 hr virus inoculation step and for an additional 2 hr and then removed ("entry"); or (c) added after the inoculation step and present for the remaining 22 hr of infection ("post-entry"). CLQ, a known modulator of intracellular pH that inhibits virus entry (Akpovwa, 2016), was recently reported to inhibit SARS-CoV-2 (Liu et al., 2020a; Wang et al., 2020a), and we confirmed its activity in the early stages of infection (Figure 3B, lane 5). Since this assay allows multiple rounds of re-infection, entry inhibitors can show antiviral effects when added post-entry as in protocol (c) (Figure 3B, lane 6). RDV was previously reported to inhibit the process for intracellular viral replication (Wang et al., 2020a), and we confirmed this mode of action showing a reduction in viral RNA levels with a negligible effect on virus entry (Figure 3B, lane 8). This assay identified that CEP targeted the virus entry phase (Figure 3B, lanes 11) while NFV clearly inhibited the post-entry process (Figure 3B, lanes 15).

Cepharanthine inhibits SARS-CoV-2 binding

In silico docking simulation shows that CEP molecules can bind the SARS-CoV-2 spike (S) protein and interfere with S engagement to its receptor, angiotensin-converting enzyme 2 (ACE2) (Lan et al., 2020; Walls et al., 2020; Wang et al., 2020b) (Figure 4A, green stick: CEP molecule, orange: S, semi-transparent cyan: ACE2). The docking model suggests that the NH of the piperidine ring of CEP molecules forms a hydrogen bond with the side chain carboxyl group of Glu484 and the backbone carbonyl group of Ser494, and the aromatic rings are in close contact with the aromatic residues (Tyr449, Tyr453, Tyr489, and Phe490) at the binding interface with ACE2. Binding free energy of CEP molecules was estimated as −24.26 kcal/mol using

[13]Center for Research and Education on Drug Discovery, Faculty of Pharmaceutical Sciences, Hokkaido University, Sapporo 060-0812, Japan

[14]Department of Virology, Faculty of Medicine, Kyushu University, Fukuoka 812-8582, Japan

[15]Department of Virology I, National Institute of Infectious Diseases, Tokyo 162-8640, Japan

[16]Department of Epidemiology and Biostatistics, Indiana University School of Public Health-Bloomington, Bloomington, IN 47405, USA

[17]National Center for Global Health and Medicine, Tokyo 162-8655, Japan

[18]Faculty of Pharmaceutical Sciences, Tokyo University of Science, Noda 278-8510, Japan

[19]Research Institute for Science and Technology, Tokyo University of Science, Noda 278-8510, Japan

[20]Department of Pathology, National Institute of Infectious Diseases, Tokyo 162-8640, Japan

[21]Laboratory of Biomolecular Science, Faculty of Pharmaceutical Sciences, Hokkaido University, Sapporo 060-0812, Japan

[22]Global Station for Biosurfaces and Drug Discovery, Center for Life Innovation, Hokkaido University, Sapporo 060-0812, Japan

[23]International Research Center for Neurointelligence, The University of Tokyo Institutes for Advanced Study, The University of Tokyo, Tokyo 113-8654, Japan

[24]Institute for the Advanced Study of Human Biology (ASHBi), Kyoto University, Kyoto 606-8501, Japan

[25]NEXT-Ganken Program, Japanese Foundation for Cancer Research (JFCR), Tokyo 135-8550, Japan

[26]Science Groove Inc., Fukuoka 810-0041, Japan

[27]Department of Virology III, National Institute of Infectious Diseases, Tokyo 208-0011, Japan

[28]Nuffield Department of Medicine, University of Oxford, Oxford OX3 7FZ, UK

[29]Research Center for Drug and Vaccine Development, National Institute of

Continued

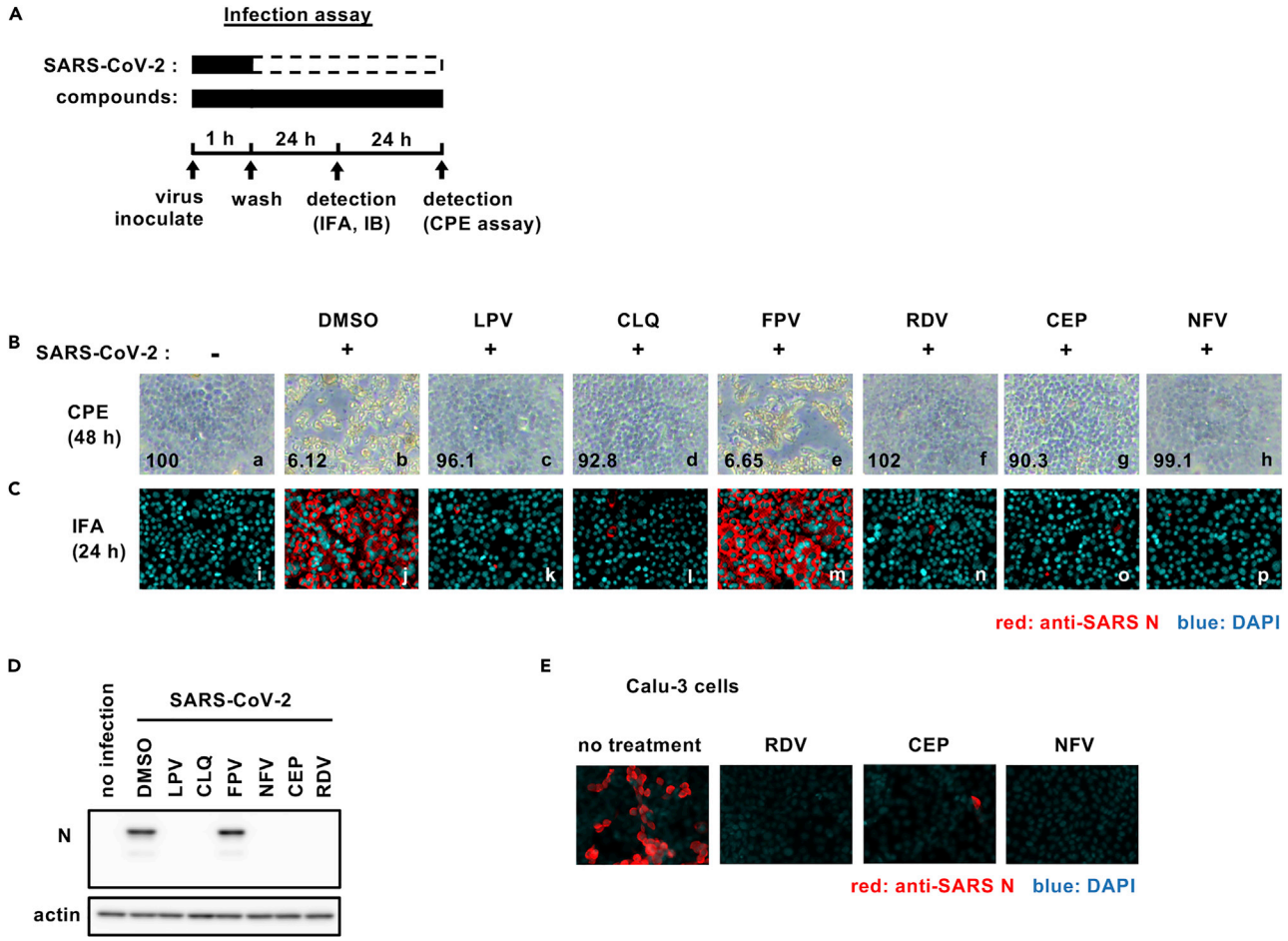

Figure 1. Cepharanthine (CEP) and nelfinavir (NFV) inhibit SARS-CoV-2 infection

(A) Schematic of the SARS-CoV-2 infection assay. VeroE6/TMPRSS2 cells were inoculated with SARS-CoV-2 in the presence of compounds. After washing out unbound virus, the cells were incubated with compounds for 24-48 hr. Cells were harvested for immunofluorescence (IFA) or immunoblot analyses of viral N protein at 24 hr, and cytopathic effects (CPEs) were observed at 48 hr after infection. Solid and dashed boxes indicate the periods with and without treatment, respectively.

(B–E) (B) Virus-induced CPE following drug treatment was recorded at 48 hr after infection. The quantified survival cell numbers (relative percentage to the control) are also shown at the bottom. Immunofluorescence (C) and immunoblot (D) detection of viral N protein expression in the infected cells at 24 hr after infection, and the red and blue signals show N and DAPI, respectively.

(E) Immunofluorescent detection of viral N protein in human lung epithelial-derived cell line, Calu-3 cells. Dimethyl sulfoxide (DMSO), 0.4%; lopinavir (LPV), 16 μM; chloroquine (CLQ), 16 μM; favipiravir (FPV), 32 μM; remdesivir (RDV), 20 μM (C and D) and 10 μM (B and E); CEP, 8 μM; NFV, 4 μM (B-D) and 8 μM (E). These data were from three independent experiments.

molecular mechanics generalized Born surface area calculation (Schrödinger, LLC). To assess this model, we investigated whether CEP inhibits SARS-CoV-2 particle binding to the cell surface or subsequent internalization into cells. We measured viral binding to cells by pre-chilling cells to prevent particle endocytosis and quantified cell-bound virus particles by quantitative PCR (qPCR) of viral RNA. CEP significantly inhibited SARS-CoV-2 binding to cells, whereas CLQ that targets intracellular trafficking pathways (Liu et al., 2020a) had a negligible effect (Figures 4B and S1). Viruses frequently exploit cellular heparan sulfate proteoglycans to initiate cell attachment, and heparin shows broad-spectrum inhibition of virus-cell attachment (De Clercq, 1998; Lang et al., 2011). As expected, heparin significantly blocked SARS-CoV-2 particle attachment to the cells (Figure 4B). These data demonstrate that CEP inhibits SARS-CoV-2 particle binding to cells.

Nelfinavir potently targets SARS-CoV-2 main protease

We conducted *in silico* docking simulation screenings to identify compounds from an approved library that interact with the SARS-CoV-2-encoded main protease (methods). Interestingly, NFV was identified among

Infectious Diseases, Tokyo 162-8640, Japan

[30]These authors contributed equally

[31]Lead contact

*Correspondence: kwatashi@nih.go.jp

https://doi.org/10.1016/j.isci.2021.102367

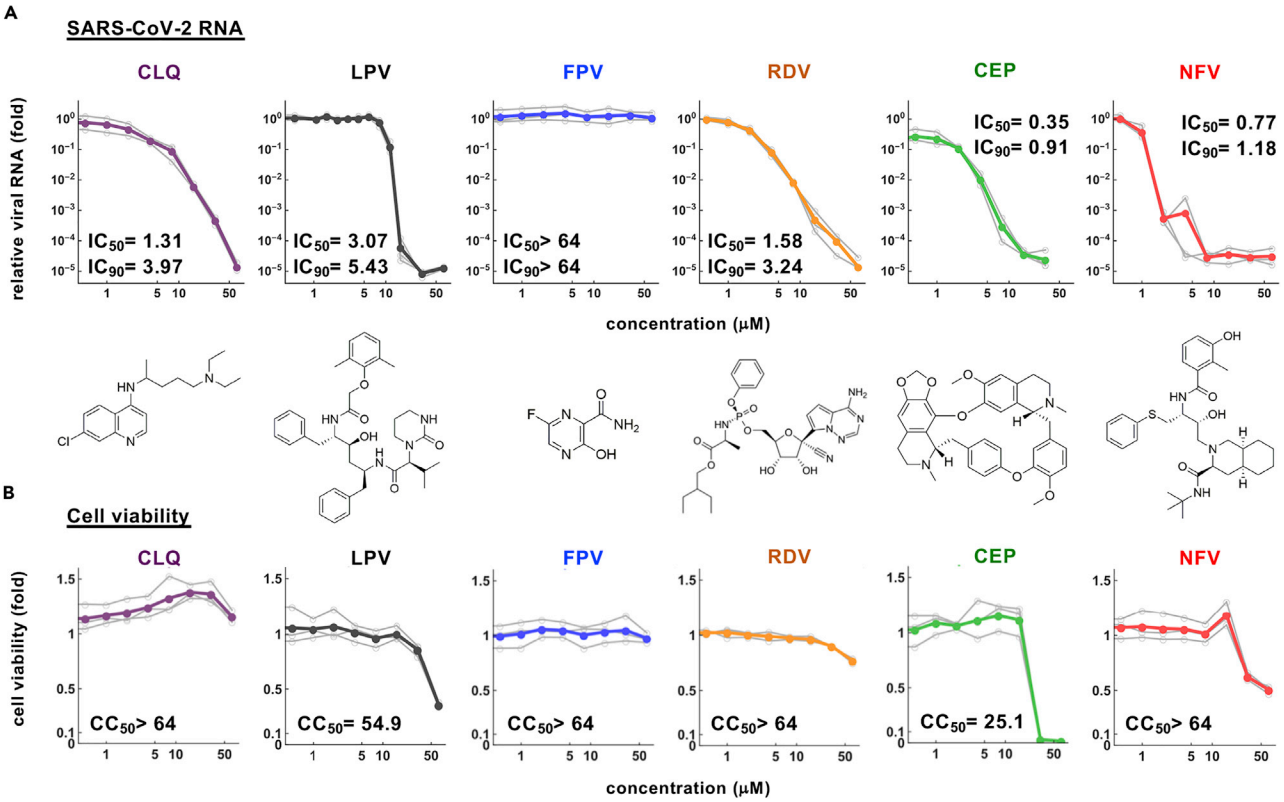

Figure 2. Dose-response curves for the antiviral activity of CEP and NFV

(A and B) Dose-response curves for compounds. In (A), secreted viral RNA at 24 hr after inoculation was quantified and plotted against drug concentration and chemical structures shown below each graph (for CEP, the structure of the major component is shown). In (B), viability of cells treated with the compounds was quantified by MTT assay. IC_{50}, IC_{90}, and CC_{50} values were estimated by median effect model and are shown. These data were from three independent experiments.

the top 1.5% ranking compounds (Figure 5A, cyan stick: NFV, green: main protease). Our docking model predicts that NFV interacts with the SARS-CoV-2 protease active site pocket and would block substrate recruitment (Figure 5A). To assess this model, we evaluated the activity of recombinant SARS-CoV-2 main protease using an *in vitro* protease assay (methods). We showed that NFV inhibited the catalytic activity of the SARS-CoV-2-encoded main protease in a dose-dependent manner, and its IC_{50} was calculated to be 37 μM (Figure 5B). These *in vitro* and *in silico* data suggest that NFV potentially targets the main protease, but its inhibition activity is likely to be weaker than that to block SARS-CoV-2 replication.

Synergy between cepharanthine and nelfinavir in blocking SARS-CoV-2 infection

Both CEP and NFV show anti-SARS-CoV-2 activity at the concentration ranges observed in patients, where the serum C_{max} of both drugs is 2.3 and 6.9 μM (by administration of 500 mg NFV orally and of 100 mg CEP by intravenous injection), respectively (Markowitz et al., 1998; Yasuda et al., 1989). Since CEP and NFV have different mode of actions, we examined their potential for synergistic effects. Antiviral activity and cell viability were determined by qPCR enumeration of viral RNA and MTT activity, respectively, following treatment with each compound alone or in combination (Figures 6A and 6B). For these experiments, we infected cells with lower amounts of SARS-CoV-2 (MOI = 0.001) and treated compounds at more frequent points of concentrations than those used in our earlier assay, for securing an accurate estimation. Single treatment with CEP (see white bars in Figure 6A) or NFV (see bars at CEP 0 μM) reduced viral RNA in a dose-dependent manner and co-treatment further reduced viral RNA levels (Figure 6A): e.g. CEP (3.20 μM) or NFV (2.24 μM) alone reduced viral RNA to 6.3% or 5.8% of untreated control, respectively, however, when combined they reduced viral RNA level to 0.068%. Higher doses of the CEP/NFV combination (4 μM each) reduced the viral RNA to undetectable levels. We compared the observed experimental antiviral activity (Figures 6A and S2A) with theoretical predictions calculated using a classical Bliss independence method

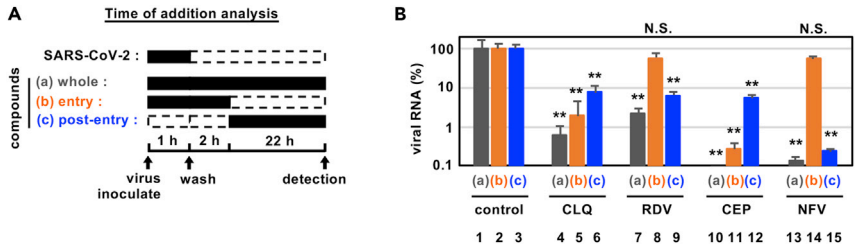

Figure 3. Antiviral mechanism of action for CEP and NFV

(A and B) Time-of-addition analysis to examine steps in SARS-CoV-2 life cycle. (A) shows the schematic of the time-of-addition analysis. Compounds were added at different times (a, whole; b, entry; or c, post-entry): (A) presentation during the 1h virus inoculation step and maintained throughout the 24 hr infection period (whole life cycle); (B) present during the 1 hr virus inoculation step and for an additional 2 hr and then removed (entry); or (C) added after the inoculation step and present for the remaining 22 hr of infection (post-entry). Solid and dashed boxes indicate the periods with and without treatment, respectively. In (B), the antiviral activities of each compound under the various protocols are estimated by quantifying the levels of secreted viral RNA at 24 hr after inoculation (B; mean ± SD). RDV, 15 μM; CLQ, 15 μM; CEP, 8.2 μM; NFV, 4 μM. These data were from three independent experiments. **P < 0.01; N.S., not significant (Student's t-test)

that assumes drugs act independently (Note S1, Figure S2B) (Greco et al., 1995; Koizumi and Iwami, 2014). The difference between the observed values and theoretical predictions suggests that CEP and NFV exhibit a synergistic activity over a broad range of concentrations (Figure 6C red: synergistic effect).

Mathematical modeling for the impact of cepharanthine and nelfinavir on SARS-CoV-2 dynamics in clinical settings

Combining the published human clinical pharmacokinetics information for these drugs (Markowitz et al., 1998; Yasuda et al., 1989; Yokoshima et al., 1986) with our observed dose-dependent antiviral data, we can calculate the antiviral activity at the time after administration (Figure 7A: left, NFV oral; center, CEP intravenous drip; right: CEP oral). Here, we used the reported pharmacokinetic information for drug distribution in the lung as well as the time-dependent drug concentration in plasma and assumed that antiviral activity depends on drug concentration in the lung (Ford et al., 2004; Shetty et al., 1996; Twigg et al., 2010) (see supplemental information in detail). Based on the time-dependent antiviral activity of drug, we can model the impact on viral burden following drug administration (Figure 7B, Note S1, Figure S3). From the viral dynamics data in Figure 7B, we calculated the cumulative viral RNA burden (i.e., area under the curve of viral load) (Figure 7C, upper) and the time required to reduce the viral load to undetectable levels (Figure 7C, lower). Our modeling predicts that NFV monotherapy would reduce the cumulative viral load by 92.1% (Figure 7C, upper, red) and would require 10.3 days to eliminate virus (Figure 7B, upper left, red), 4.9 days shorter than untreated controls (Figure 7C, lower, red). In contrast, orally administered CEP shows a minimal effect on the viral load (Figure 7B, lower left, green), most likely reflecting low drug concentrations, while intravenous delivery of CEP reduces the cumulative viral load (Figures 7B and 7C, green) and shortens the period for virus elimination (Figure 7C, lower, green) because of achieving enough drug concentration (see Discussion). Importantly, co-administering NFV (oral) and CEP (intravenous drip) resulted in a more rapid decline in viral RNA, with undetectable levels 6.15 days earlier than untreated controls and 1.23 days earlier than NFV alone (Figure 7C, orange). Another advantage of combination treatment is discussed in discussion. In summary, our prediction shows the potential antiviral efficacy of NFV and CEP and its combined treatment that facilitates SARS-CoV-2 elimination.

DISCUSSION

Screening a panel of approved drugs identified two agents, CEP and NFV, that inhibit SARS-CoV-2 infection with the highest potencies in our screening. A recent study reported that CEP showed anti-SARS-CoV-2 activity, and the authors speculated that CEP targeted both entry and viral replication phase of the virus life cycle (Fan et al., 2020; Jeon et al., 2020). However, our time-of-addition studies along with viral binding and docking simulation analysis suggest that CEP predominantly inhibits virus-cell binding. We also have preliminary data by surface plasmon resonance analysis showing a potential interaction between CEP and the S protein, speculating its mode of action and which needs to be further analyzed in the future. These data are consistent with a previous paper reporting that CEP reduced the entry of another human

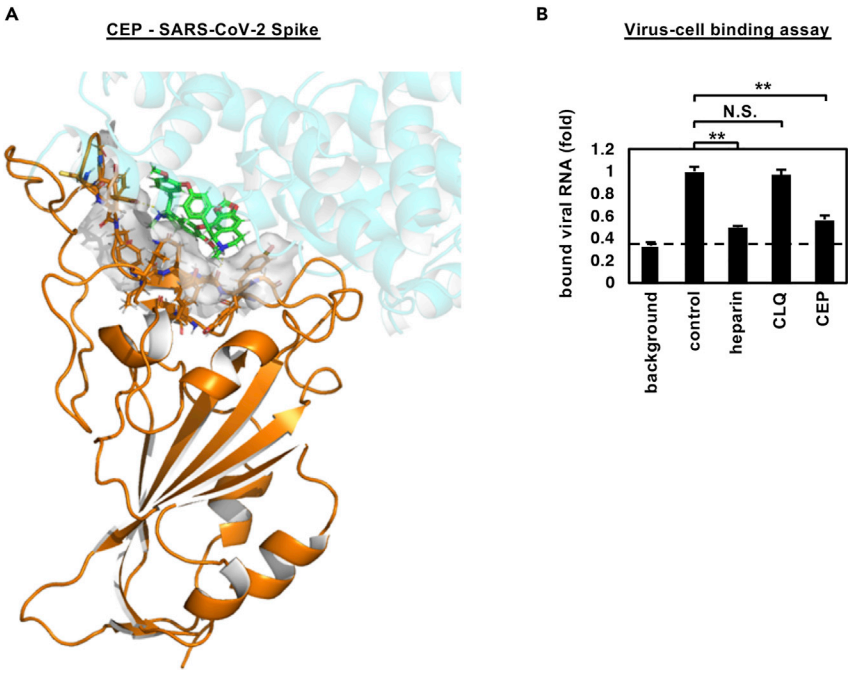

Figure 4. CEP inhibits SARS-CoV-2 cell binding

(A) Predicted binding of CEP molecule to SARS-CoV-2 spike protein. Spike protein, CEP molecule, and protein binding site residues around CEP within 4 Å are shown in cartoon representation colored in orange, green stick, and surface representation, respectively. An overlapping view of the ACE2 with CEP is shown in semi-transparent cartoon representation colored in cyan.

(B) Virus-cell binding assay. VeroE6/TMPRSS2 cells were incubated with virus (MOI = 0.001) in the presence of the indicated compounds for 30 min at 4°C to allow virus-cell binding. After extensive washing, cell-bound viral RNA was quantified, where the background depicts residual viral inocula in the absence of cells (B; mean ± SD). These data were from three independent experiments. **$p < 0.01$; N.S., not significant (Student's t-test)

coronavirus OC43 (Kim et al., 2019). There is a significant global effort to generate a COVID-19 vaccine that will target the SARS-CoV-2 S glycoprotein (Thanh Le et al., 2020). It is worthy of future investigation to examine whether CEP is effective to augment the antiviral activity of neutralizing antibodies. After the emergence of COVID-19 pandemic, *in silico* studies have been widely conducted to seek for anti-COVID-19 drugs and NFV was predicted for a potential to associate with SARS-CoV-2 life cycle (Huynh et al., 2020; Mittal et al., 2020; Mothay and Ramesh, 2020; Musarrat et al., 2020; Reiner et al., 2020). NFV was reported to inhibit the replication of another coronavirus, SARS-CoV (Liu et al., 2005; Wu et al., 2004; Yamamoto et al., 2004). Our study is consistent with the recent report showing the anti-SARS-CoV-2 activity of NFV, which has been published during the review process of this paper, although its mode of action and the prediction of antiviral effect in clinical settings were not analyzed (Ianevski et al., 2020). In addition to the identification of anti-SARS-CoV-2 activity of NFV from a chemical screening, our study showed that NFV inhibited SARS-CoV-2 replication with under μM order and inhibited the catalytic activity of main protease with lower activity, predicted by *in silico* modeling. Our data suggest that NFV potently inhibits the main protease and also possibly targets another factor. A non-infectious cell fusion system also reported that NFV inhibited SARS-CoV-2 spike-mediated membrane fusion at the concentration of over 10 μM (Musarrat et al., 2020), providing another possible antiviral activity of NFV. In addition, the observation that CEP and NFV target different steps in the viral life cycle supports the development of multidrug combination therapies for treating COVID-19.

Our mathematical modeling studies assess how drug candidates can suppress and eliminate SARS-CoV-2. Based on the reported lung distribution/concentration of CEP and NFV in patients, we predicted that NFV at clinical doses can maintain significant antiviral effects throughout the treatment period and reduce SARS-CoV-2 RNA burden that results in shortening the time required to eliminate infection. In contrast, we predict that oral administration of CEP will have limited antiviral effect due to its low concentration

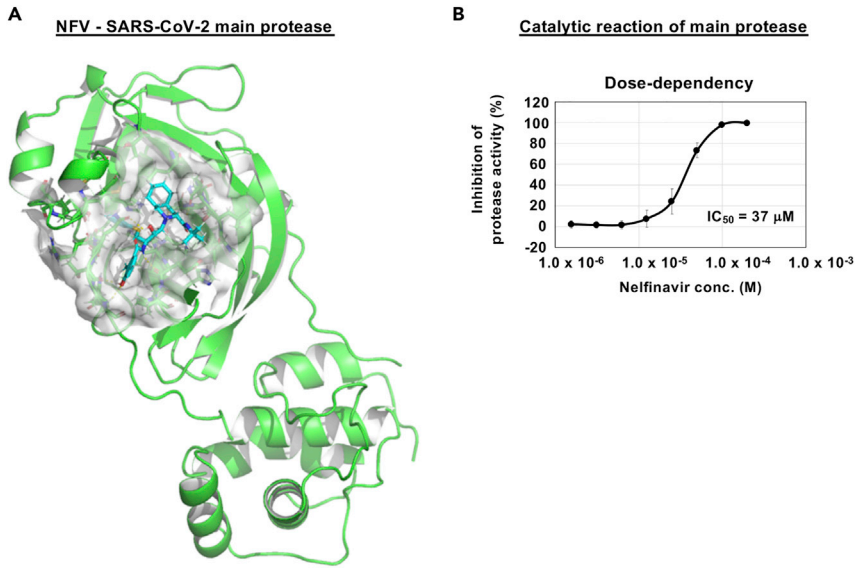

Figure 5. NFV potentially targets SARS-CoV-2 main protease

(A) Predicted binding of NFV to SARS-CoV-2 main protease. Representation of SARS-CoV-2 main protease (green), NFV molecule (cyan stick), and protease binding site residues around NFV within 4 Å (surface representation) is shown.

(B) Dose-dependent inhibition curves for NFV on the catalytic activity of the SARS-CoV-2 main protease. The IC_{50} is also shown. (B; mean ± SD)

in vivo. However, intravenous delivery of CEP achieves higher drug concentrations especially accumulated in the lung (Yokoshima et al., 1986) that enables sustained antiviral activity. It is noteworthy that combining CEP with NFV further reduced the cumulative viral load and facilitated virus elimination. As the cumulative viral load in patients is likely to associate with disease progression and risk of new transmission (Liu et al., 2020b), such multidrug treatments will be of benefit to improve clinical outcome and to control the epidemic. In addition to potentiating antiviral effects, combination treatment can limit the emergence of viral drug resistance which is frequently reported for RNA viruses such as coronavirus. Limitations of this mathematical prediction are shown in limitations of the study section; however, our analysis warrants the further clinical trial for oral NFV treatment in Japan (jRCT2071200023).

Several *in vivo* SARS-CoV-2 infection systems were recently reported: nonhuman primates, ferrets, hamsters, transgenic mice overexpressing human ACE2, and wild-type mice infected with mouse-adapted virus (Bao et al., 2020; Gao et al., 2020; Kim et al., 2020; Munster et al., 2020; Rockx et al., 2020). Given the urgency of the COVID-19 pandemic, we believe that a lack of *in vivo* validation should not preclude the clinical assessment of new antiviral agents. We here propose CEP and NFV as potential antiviral drug candidates against COVID-19, and thus, NFV is under clinical evaluation in a multicenter randomized controlled trial in Japan (jRCT2071200023).

Limitations of the study

In this study, we mainly used VeroE6/TMPRSS2 cells and applied the dose-dependent antiviral activity in these cells (Figure 2A) to predict the drug efficacy in patients (Figure 7). More physiologically relevant cell models such as primary human respiratory/lung cells in air-liquid interface culture and organoids or presumably *in vivo* infection models would be needed to strengthen the data. As well, our mathematical prediction was based on the total drug concentration in the lung, although free drug that does not non-specifically bind to proteins is believed to be pharmacologically active. There is no information available on the free CEP and NFV concentration in the lung tissue.

Resource availability

Lead contact

Further information and requests for resources and reagents should be directed to and will be fulfilled by the lead contact, Koichi Watashi: kwatashi@nih.go.jp.

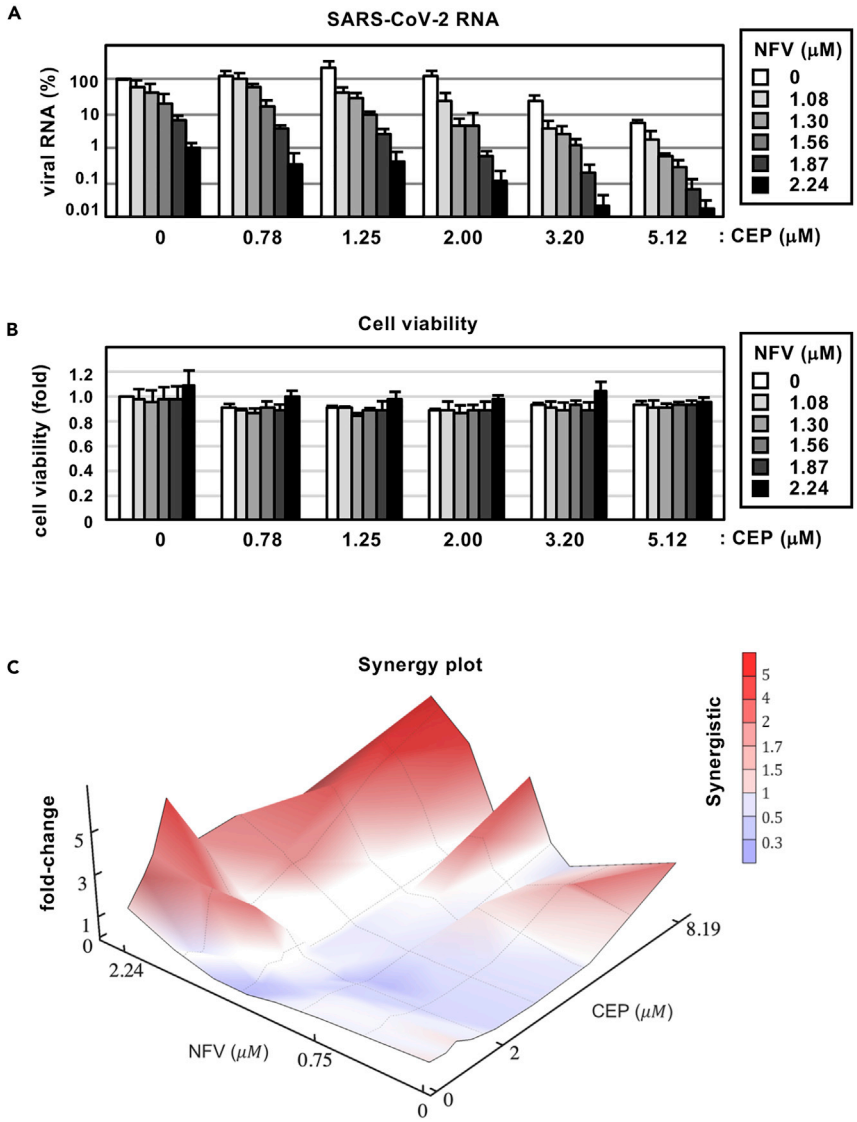

Figure 6. Combination treatment with CEP and NFV

(A) Dose-response curve of CEP/NFV co-treatment in the infection experiment (MOI = 0.001). Extracellular viral RNA levels at 24 hr after infection were quantified and plotted against concentrations of CEP (0.78, 1.25, 2.00, 3.20, and 5.12 μM: 1.6-fold serial dilution) and NFV (1.08, 1.30, 1.56, 1.87, and 2.24 μM: 1.2-fold serial dilution).

(B) Cell viability upon co-treatment with compounds.

(C) The three-dimensional interaction landscapes of CEP and NFV were evaluated based on the Bliss independence model. Red and blue colors on the contour plot indicate synergy and antagonism, respectively. These data were from three independent experiments (A, B; mean ± SD).

Materials availability

This study did not generate new unique materials.

Data and code availability

All data are included in the article and supplemental information and any additional information will be available from the lead contact upon request.

METHODS

All methods can be found in the accompanying transparent methods supplemental file.

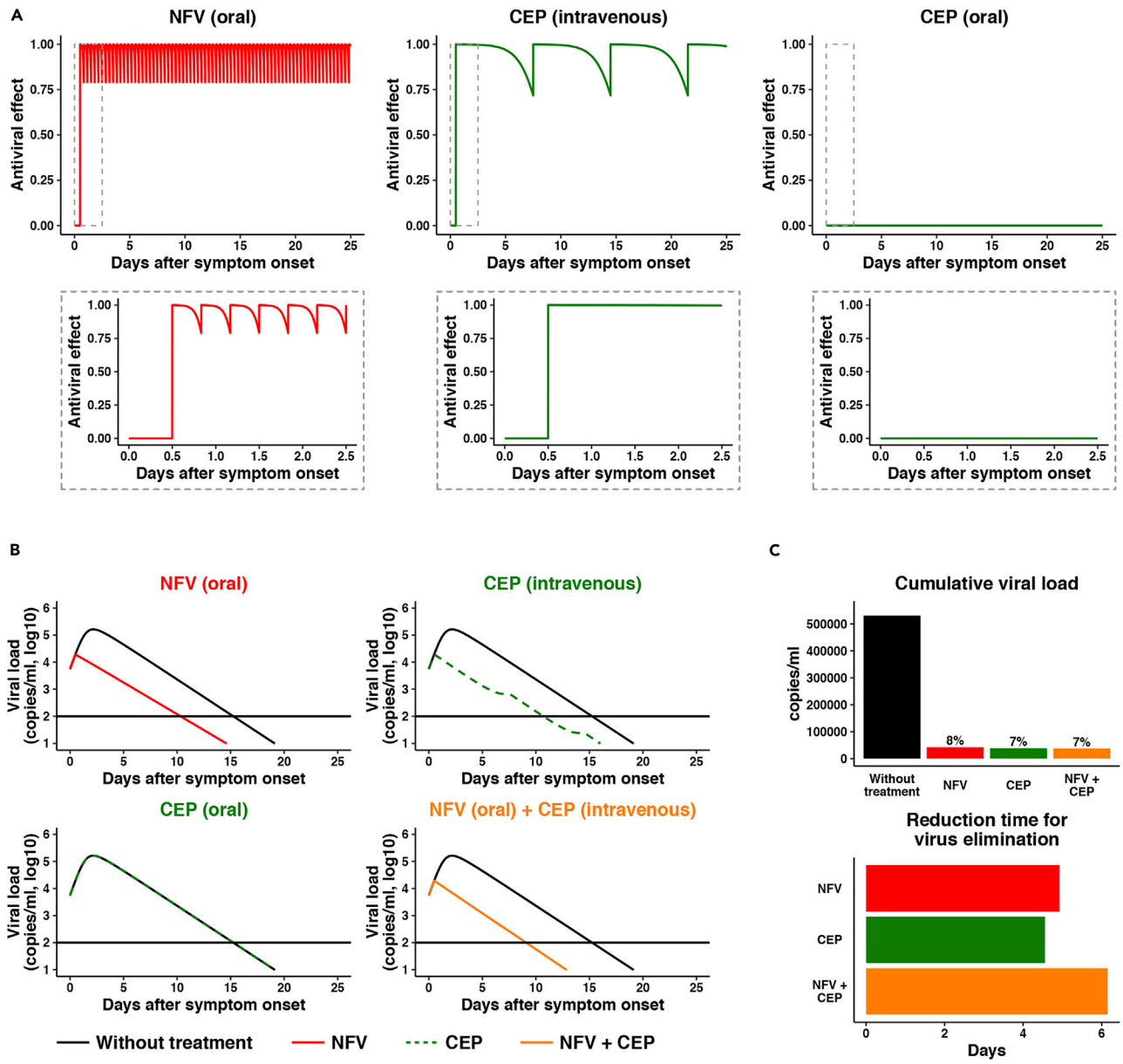

Figure 7. Mathematical prediction of the impact of CEP and NFV therapy on viral dynamics

(A) The time-dependent antiviral effects of NFV (500 mg, TID, oral) and CEP [25 mg, intravenous drip or 10 mg, oral] predicted by pharmacokinetics/pharmacodynamics (PK/PD) model are shown, with enlarged views of the gray zones in upper panels.

(B) Viral load dynamics in the presence or absence of NFV (oral), CEP (intravenous), CEP (oral), and NFV (oral)/CEP (intravenous) combined therapies predicted by pharmacokinetics/pharmacodynamics/viral dynamics (PK/PD/VD) models are shown.

(C) The cumulative antiviral load [area under the curve in (B)] (upper) and the reduction time (days) for virus elimination (lower) with drug treatments [NFV (oral), CEP (intravenous), and the NFV (oral)/CEP (intravenous) combination] are shown.

SUPPLEMENTAL INFORMATION

Supplemental information can be found online at https://doi.org/10.1016/j.isci.2021.102367.

ACKNOWLEDGMENTS

We thank Drs. Shuetsu Fukushi and Souichi Yamada at the Department of Virology I, National Institute of Infectious Diseases, Satoko Otsuguro, Dr. Manabu Nagao and Sayaka Niizuma at Hokkaido University, and Noriko Kurisaki at Kyushu University for technical assistance. NFV, LPV, and FPV were kindly provided by

Japan Tobacco, Abbvie, and Fujifilm Toyama Chemical. Pharmaceutical preparation of CEP was kindly provided by Medisa Shinyaku Inc, a subsidiary of Sawai Pharmaceutical. This work was supported by the Agency for Medical Research and Development (AMED) emerging/re-emerging infectious diseases project (JP19fk0108111, JP19fk0108110, JP20fk0108104, JP20fk0108411); the AMED Basis for Supporting Innovative Drug Discovery and Life Science Research (BINDS, JP19am0101114, JP19am0101069, JP19am0101111) program; the Japan Society for the Promotion of Science KAKENHI (JP17H04085, JP20H03499, JP15H05707, 19H04839); the JST MIRAI Program; and the Wellcome Trust-funded Investigator award (200838/Z/16/Z).

AUTHOR CONTRIBUTIONS

Conceptualization, K.W.; investigation, H.O., K.W., W.S., K.S., S. Iwanami, T.H., T. Shirai., S.K., Y.I., K.S.K., T.N., Tateki Suzuki, K.N., and S. Iwami; methodology and resources, S.Ando., Tadaki Suzuki., T.H., K.M., M.S., M.T., T.W.; analysis, all the authors; writing and editing, K.W., T.H., K.A., S. Iwami, and J.A.M; funding acquisition, K.W. and M.T.; supervision, K.W.

DECLARATION OF INTERESTS

The authors declare no competing interests.

Received: June 7, 2020
Revised: November 2, 2020
Accepted: March 24, 2021
Published: April 23, 2021

REFERENCES

Akpovwa, H. (2016). Chloroquine could be used for the treatment of filoviral infections and other viral infections that emerge or emerged from viruses requiring an acidic pH for infectivity. Cell Biochem. Funct. *34*, 191–196, https://doi.org/10.1002/cbf.3182.

Bailly, C. (2019). Cepharanthine: an update of its mode of action, pharmacological properties and medical applications. Phytomedicine *62*, 152956, https://doi.org/10.1016/j.phymed.2019.152956.

Bao, L., Deng, W., Huang, B., Gao, H., Liu, J., Ren, L., Wei, Q., Yu, P., Xu, Y., Qi, F., et al. (2020). The pathogenicity of SARS-CoV-2 in hACE2 transgenic mice. Nature. https://doi.org/10.1038/s41586-020-2312-y.

Beigel, J.H., Tomashek, K.M., Dodd, L.E., Mehta, A.K., Zingman, B.S., Kalil, A.C., Hohmann, E., Chu, H.Y., Luetkemeyer, A., Kline, S., et al. (2020). Remdesivir for the treatment of covid-19 - preliminary report. N. Engl. J. Med. https://doi.org/10.1056/NEJMoa2007764.

Boulware, D.R., Pullen, M.F., Bangdiwala, A.S., Pastick, K.A., Lofgren, S.M., Okafor, E.C., Skipper, C.P., Nascene, A.A., Nicol, M.R., Abassi, M., et al. (2020). A randomized trial of hydroxychloroquine as postexposure prophylaxis for covid-19. N. Engl. J. Med. https://doi.org/10.1056/NEJMoa2016638.

Cao, B., Wang, Y., Wen, D., Liu, W., Wang, J., Fan, G., Ruan, L., Song, B., Cai, Y., Wei, M., et al. (2020). A trial of lopinavir-ritonavir in adults hospitalized with severe covid-19. N. Engl. J. Med. https://doi.org/10.1056/NEJMoa2001282.

Choy, K.T., Wong, A.Y., Kaewpreedee, P., Sia, S.F., Chen, D., Hui, K.P.Y., Chu, D.K.W., Chan, M.C.W., Cheung, P.P., Huang, X., et al. (2020). Remdesivir, lopinavir, emetine, and homoharringtonine inhibit SARS-CoV-2 replication in vitro. Antivir. Res *178*, 104786, https://doi.org/10.1016/j.antiviral.2020.104786.

De Clercq, E. (1998). Virus attachment. Pharmacochem. Libr. *29*, 91–104.

Dong, L., Hu, S., and Gao, J. (2020). Discovering drugs to treat coronavirus disease 2019 (COVID-19). Drug Discov. Ther. *14*, 58–60, https://doi.org/10.5582/ddt.2020.01012.

Fan, H.H., Wang, L.Q., Liu, W.L., An, X.P., Liu, Z.D., He, X.Q., Song, L.H., and Tong, Y.G. (2020). Repurposing of clinically approved drugs for treatment of coronavirus disease 2019 in a 2019-novel coronavirus (2019-nCoV) related coronavirus model. Chin. Med. J. https://doi.org/10.1097/CM9.0000000000000797.

Ford, J., Cornforth, D., Hoggard, P.G., Cuthbertson, Z., Meaden, E.R., Williams, I., Johnson, M., Daniels, E., Hsyu, P., Back, D.J., et al. (2004). Intracellular and plasma pharmacokinetics of nelfinavir and M8 in HIV-infected patients: relationship with P-glycoprotein expression. Antivir. Ther. *9*, 77–84.

Gao, Q., Bao, L., Mao, H., Wang, L., Xu, K., Yang, M., Li, Y., Zhu, L., Wang, N., Lv, Z., et al. (2020). Rapid development of an inactivated vaccine candidate for SARS-CoV-2. Science. https://doi.org/10.1126/science.abc1932.

Greco, W.R., Bravo, G., and Parsons, J.C. (1995). The search for synergy: a critical review from a response surface perspective. Pharmacol. Rev. *47*, 331–385.

Huang, C., Wang, Y., Li, X., Ren, L., Zhao, J., Hu, Y., Zhang, L., Fan, G., Xu, J., Gu, X., et al. (2020). Clinical features of patients infected with 2019 novel coronavirus in Wuhan, China. Lancet *395*, 497–506, https://doi.org/10.1016/S0140-6736(20)30183-5.

Huynh, T., Wang, H., and Luan, B. (2020). In silico exploration of the molecular mechanism of clinically oriented drugs for possibly inhibiting SARS-CoV-2's main protease. J. Phys. Chem. Lett. *11*, 4413–4420, https://doi.org/10.1021/acs.jpclett.0c00994.

Ianevski, A., Yao, R., Fenstad, M.H., Biza, S., Zusinaite, E., Reisberg, T., Lysvand, H., Loseth, K., Landsem, V.M., Malmring, J.F., et al. (2020). Potential antiviral options against SARS-CoV-2 infection. Viruses *12*, https://doi.org/10.3390/v12060642.

Jeon, S., Ko, M., Lee, J., Choi, I., Byun, S.Y., Park, S., Shum, D., and Kim, S. (2020). Identification of antiviral drug candidates against SARS-CoV-2 from FDA-approved drugs. Antimicrob. Agents Chemother. *64*, https://doi.org/10.1128/AAC.00819-20.

Kao, M.C., Yang, C.H., Sheu, J.R., and Huang, C.J. (2015). Cepharanthine mitigates pro-inflammatory cytokine response in lung injury induced by hemorrhagic shock/resuscitation in rats. Cytokine *76*, 442–448, https://doi.org/10.1016/j.cyto.2015.09.008.

Kim, D.E., Min, J.S., Jang, M.S., Lee, J.Y., Shin, Y.S., Song, J.H., Kim, H.R., Kim, S., Jin, Y.H., and Kwon, S. (2019). Natural bis-benzylisoquinoline alkaloids-tetrandrine, fangchinoline, and cepharanthine, inhibit human coronavirus OC43 infection of MRC-5 human lung cells. Biomolecules *9*, https://doi.org/10.3390/biom9110696.

Kim, Y.I., Kim, S.G., Kim, S.M., Kim, E.H., Park, S.J., Yu, K.M., Chang, J.H., Kim, E.J., Lee, S., Casel, M.A.B., et al. (2020). Infection and rapid

transmission of SARS-CoV-2 in ferrets. Cell Host Microbe. https://doi.org/10.1016/j.chom.2020.03.023.

Koizumi, Y., and Iwami, S. (2014). Mathematical modeling of multi-drugs therapy: a challenge for determining the optimal combinations of antiviral drugs. Theor. Biol. Med. Model. *11*, 41, https://doi.org/10.1186/1742-4682-11-41.

Lan, J., Ge, J., Yu, J., Shan, S., Zhou, H., Fan, S., Zhang, Q., Shi, X., Wang, Q., Zhang, L., et al. (2020). Structure of the SARS-CoV-2 spike receptor-binding domain bound to the ACE2 receptor. Nature. https://doi.org/10.1038/s41586-020-2180-5.

Lang, J., Yang, N., Deng, J., Liu, K., Yang, P., Zhang, G., and Jiang, C. (2011). Inhibition of SARS pseudovirus cell entry by lactoferrin binding to heparan sulfate proteoglycans. PLoS One *6*, e23710, https://doi.org/10.1371/journal.pone.0023710.

Liu, J., Cao, R., Xu, M., Wang, X., Zhang, H., Hu, H., Li, Y., Hu, Z., Zhong, W., and Wang, M. (2020a). Hydroxychloroquine, a less toxic derivative of chloroquine, is effective in inhibiting SARS-CoV-2 infection in vitro. Cell Discov. *6*, 16, https://doi.org/10.1038/s41421-020-0156-0.

Liu, Y., Yan, L.M., Wan, L., Xiang, T.X., Le, A., Liu, J.M., Peiris, M., Poon, L.L.M., and Zhang, W. (2020b). Viral dynamics in mild and severe cases of COVID-19. Lancet Infect. Dis. https://doi.org/10.1016/S1473-3099(20)30232-2.

Liu, Y.C., Huang, V., Chao, T.C., Hsiao, C.D., Lin, A., Chang, M.F., and Chow, L.P. (2005). Screening of drugs by FRET analysis identifies inhibitors of SARS-CoV 3CL protease. Biochem. Biophys. Res. Commun. *333*, 194–199, https://doi.org/10.1016/j.bbrc.2005.05.095.

Markowitz, M., Conant, M., Hurley, A., Schluger, R., Duran, M., Peterkin, J., Chapman, S., Patick, A., Hendricks, A., Yuen, G.J., et al. (1998). A preliminary evaluation of nelfinavir mesylate, an inhibitor of human immunodeficiency virus (HIV)-1 protease, to treat HIV infection. J. Infect. Dis. *177*, 1533–1540, https://doi.org/10.1086/515312.

Matsuyama, S., Nao, N., Shirato, K., Kawase, M., Saito, S., Takayama, I., Nagata, N., Sekizuka, T., Katoh, H., Kato, F., et al. (2020). Enhanced isolation of SARS-CoV-2 by TMPRSS2-expressing cells. Proc. Natl. Acad. Sci. U S A *117*, 7001–7003, https://doi.org/10.1073/pnas.2002589117.

Mittal, L., Kumari, A., Srivastava, M., Singh, M., and Asthana, S. (2020). Identification of potential molecules against COVID-19 main protease through structure-guided virtual screening approach. J. Biomol. Struct. Dyn. 1–19, https://doi.org/10.1080/07391102.2020.1768151.

Mothay, D., and Ramesh, K.V. (2020). Binding site analysis of potential protease inhibitors of COVID-19 using AutoDock. VirusDisease, 1–6, https://doi.org/10.1007/s13337-020-00585-z.

Munster, V.J., Feldmann, F., Williamson, B.N., van Doremalen, N., Perez-Perez, L., Schulz, J., Meade-White, K., Okumura, A., Callison, J., Brumbaugh, B., et al. (2020). Respiratory disease in rhesus macaques inoculated with SARS-CoV-2. Nature. https://doi.org/10.1038/s41586-020-2324-7.

Musarrat, F., Chouljenko, V., Dahal, A., Nabi, R., Chouljenko, T., Jois, S.D., and Kousoulas, K.G. (2020). The anti-HIV drug nelfinavir mesylate (Viracept) is a potent inhibitor of cell fusion caused by the SARSCoV-2 spike (S) glycoprotein warranting further evaluation as an antiviral against COVID-19 infections. J. Med. Virol. https://doi.org/10.1002/jmv.25985.

Pizzorno, A., Padey, B., Dubois, J., Julien, T., Traversier, A., Duliere, V., Brun, P., Lina, B., Rosa-Calatrava, M., and Terrier, O. (2020). In vitro evaluation of antiviral activity of single and combined repurposable drugs against SARS-CoV-2. Antivir. Res, 104878, https://doi.org/10.1016/j.antiviral.2020.104878.

Reiner, Z., Hatamipour, M., Banach, M., Pirro, M., Al-Rasadi, K., Jamialahmadi, T., Radenkovic, D., Montecucco, F., and Sahebkar, A. (2020). Statins and the COVID-19 main protease: in silico evidence on direct interaction. Arch. Med. Sci. *16*, 490–496, https://doi.org/10.5114/aoms.2020.94655.

Rockx, B., Kuiken, T., Herfst, S., Bestebroer, T., Lamers, M.M., Oude Munnink, B.B., de Meulder, D., van Amerongen, G., van den Brand, J., Okba, N.M.A., et al. (2020). Comparative pathogenesis of COVID-19, MERS, and SARS in a nonhuman primate model. Science *368*, 1012–1015, https://doi.org/10.1126/science.abb7314.

Shetty, B.V., Kosa, M.B., Khalil, D.A., and Webber, S. (1996). Preclinical pharmacokinetics and distribution to tissue of AG1343, an inhibitor of human immunodeficiency virus type 1 protease. Antimicrob. Agents Chemother. *40*, 110–114, https://doi.org/10.1128/AAC.40.1.110.

Thanh Le, T., Andreadakis, Z., Kumar, A., Gomez Roman, R., Tollefsen, S., Saville, M., and Mayhew, S. (2020). The COVID-19 vaccine development landscape. Nat. Rev. Drug Discov. https://doi.org/10.1038/d41573-020-00073-5.

Touret, F., and de Lamballerie, X. (2020). Of chloroquine and COVID-19. Antivir. Res *177*, 104762, https://doi.org/10.1016/j.antiviral.2020.104762.

Twigg, H.L., Schnizlein-Bick, C.T., Weiden, M., Valentine, F., Wheat, J., Day, R.B., Rominger, H., Zheng, L., Collman, R.G., Coombs, R.W., et al. (2010). Measurement of antiretroviral drugs in the lungs of HIV-infected patients. HIV Ther. *4*, 247–251, https://doi.org/10.2217/hiv.10.5.

Walls, A.C., Park, Y.J., Tortorici, M.A., Wall, A., McGuire, A.T., and Veesler, D. (2020). Structure, function, and antigenicity of the SARS-CoV-2 spike glycoprotein. Cell. https://doi.org/10.1016/j.cell.2020.02.058.

Wang, M., Cao, R., Zhang, L., Yang, X., Liu, J., Xu, M., Shi, Z., Hu, Z., Zhong, W., and Xiao, G. (2020a). Remdesivir and chloroquine effectively inhibit the recently emerged novel coronavirus (2019-nCoV) in vitro. Cell Res *30*, 269–271, https://doi.org/10.1038/s41422-020-0282-0.

Wang, Q., Zhang, Y., Wu, L., Niu, S., Song, C., Zhang, Z., Lu, G., Qiao, C., Hu, Y., Yuen, K.Y., et al. (2020b). Structural and functional Basis of SARS-CoV-2 entry by using human ACE2. Cell. https://doi.org/10.1016/j.cell.2020.03.045.

WHO (2020) Coronavirus disease (COVID-19) pandemic. https://www.who.int/emergencies/diseases/novel-coronavirus-2019.

Wu, C.Y., Jan, J.T., Ma, S.H., Kuo, C.J., Juan, H.F., Cheng, Y.S., Hsu, H.H., Huang, H.C., Wu, D., Brik, A., et al. (2004). Small molecules targeting severe acute respiratory syndrome human coronavirus. Proc. Natl. Acad. Sci. U S A *101*, 10012–10017, https://doi.org/10.1073/pnas.0403596101.

Yamamoto, N., Yang, R., Yoshinaka, Y., Amari, S., Nakano, T., Cinatl, J., Rabenau, H., Doerr, H.W., Hunsmann, G., Otaka, A., et al. (2004). HIV protease inhibitor nelfinavir inhibits replication of SARS-associated coronavirus. Biochem. Biophys. Res. Commun. *318*, 719–725, https://doi.org/10.1016/j.bbrc.2004.04.083.

Yasuda, K., Moro, M., Akasu, M., and Ohnishi, A. (1989). Pharmacokinetic disposition of cepharanthin following single and multiple intravenous doses in healthy subjects. Jpn. J. Clin. Pharmacol. Ther. *20*, 741–749.

Yokoshima, T., Tsutsumi, S., Ohtsuki, T., Takaichi, M., Nakajima, T., and Akasu, M. (1986). Studies on metabolic fate of cepharanthine: absorption, distribution, metabolism and excretion in rats. Pharm. Regul. Sci. *17*, 458–479.

Zhou, P., Yang, X.L., Wang, X.G., Hu, B., Zhang, L., Zhang, W., Si, H.R., Zhu, Y., Li, B., Huang, C.L., et al. (2020). A pneumonia outbreak associated with a new coronavirus of probable bat origin. Nature *579*, 270–273, https://doi.org/10.1038/s41586-020-2012-7.

Zhu, N., Zhang, D., Wang, W., Li, X., Yang, B., Song, J., Zhao, X., Huang, B., Shi, W., Lu, R., et al. (2020). A novel coronavirus from patients with pneumonia in China, 2019. N. Engl. J. Med. *382*, 727–733, https://doi.org/10.1056/NEJMoa2001017.

iScience, Volume *24*

Supplemental information

Potential anti-COVID-19 agents, cepharanthine and nelfinavir, and their usage for combination treatment

Hirofumi Ohashi, Koichi Watashi, Wakana Saso, Kaho Shionoya, Shoya Iwanami, Takatsugu Hirokawa, Tsuyoshi Shirai, Shigehiko Kanaya, Yusuke Ito, Kwang Su Kim, Takao Nomura, Tateki Suzuki, Kazane Nishioka, Shuji Ando, Keisuke Ejima, Yoshiki Koizumi, Tomohiro Tanaka, Shin Aoki, Kouji Kuramochi, Tadaki Suzuki, Takao Hashiguchi, Katsumi Maenaka, Tetsuro Matano, Masamichi Muramatsu, Masayuki Saijo, Kazuyuki Aihara, Shingo Iwami, Makoto Takeda, Jane A. McKeating, and Takaji Wakita

Supplemental Information

Potential anti-COVID-19 agents, Cepharanthine and Nelfinavir, and their usage for combination treatment

Hirofumi Ohashi[1,2,¶], Koichi Watashi[1,2,3,4,29,¶*], Wakana Saso[1,5.6,¶], Kaho Shionoya[1,2], Shoya Iwanami[7], Takatsugu Hirokawa[8,9,10], Tsuyoshi Shirai[11], Shigehiko Kanaya[12], Yusuke Ito[7], Kwang Su Kim[7], Takao Nomura[13], Tateki Suzuki[14], Kazane Nishioka[1,2], Shuji Ando[15], Keisuke Ejima[16], Yoshiki Koizumi[17], Tomohiro Tanaka[18], Shin Aoki[18,19], Kouji Kuramochi[2], Tadaki Suzuki[20], Takao Hashiguchi[14], Katsumi Maenaka[13,21,22], Tetsuro Matano[5,6], Masamichi Muramatsu[1], Masayuki Saijo[15], Kazuyuki Aihara[23], Shingo Iwami[4,7,24,25,26], Makoto Takeda[27], Jane A. McKeating[28], Takaji Wakita[1]

[1]Department of Virology II, National Institute of Infectious Diseases, Tokyo 162-8640, Japan,
[2]Department of Applied Biological Science, Tokyo University of Science, Noda 278-8510, Japan,
[3]Institute for Frontier Life and Medical Sciences, Kyoto University, Kyoto 606-8507, Japan,
[4]MIRAI, JST, Saitama 332-0012, Japan,
[5]The Institute of Medical Science, The University of Tokyo, Tokyo 108-8639, Japan,
[6]AIDS Research Center, National Institute of Infectious Diseases, Tokyo 162-8640, Japan,
[7]Department of Biology, Faculty of Sciences, Kyushu University, Fukuoka 812-8581, Japan,
[8]Cellular and Molecular Biotechnology Research Institute, National Institute of Advanced Industrial Science and Technology, Tokyo 135-0064, Japan,
[9]Division of Biomedical Science, Faculty of Medicine, University of Tsukuba, Tsukuba 305-8575, Japan,
[10]Transborder Medical Research Center, University of Tsukuba, Tsukuba 305-8575, Japan,
[11]Faculty of Bioscience, Nagahama Institute of Bio-Science and Technology, Nagahama 526-0829, Japan,
[12]Graduate School of Science and Technology, Nara Institute of Science and Technology, Ikoma 630-0192, Japan,
[13]Center for Research and Education on Drug Discovery, Faculty of Pharmaceutical Sciences, Hokkaido University, Sapporo 060-0812, Japan,
[14]Department of Virology, Faculty of Medicine, Kyushu University, Fukuoka 812-8582, Japan,
[15]Department of Virology I, National Institute of Infectious Diseases, Tokyo 162-8640, Japan,
[16]Department of Epidemiology and Biostatistics, Indiana University School of Public Health-Bloomington, IN 47405, USA,
[17]National Center for Global Health and Medicine, Tokyo162-8655, Japan,
[18]Faculty of Pharmaceutical Sciences, Tokyo University of Science, Noda 278-8510, Japan,
[19]Research Institute for Science and Technology, Tokyo University of Science, Noda 278-8510, Japan,
[20]Department of Pathology, National Institute of Infectious Diseases, Tokyo 162-8640, Japan,
[21]Laboratory of Biomolecular Science, Faculty of Pharmaceutical Sciences, Hokkaido University, Sapporo 060-0812, Japan,

[22]Global Station for Biosurfaces and Drug Discovery, Center for Life Innovation, Hokkaido University, Sapporo 060-0812, Japan,
[23]International Research Center for Neurointelligence, The University of Tokyo Institutes for Advanced Study, The University of Tokyo, Tokyo 113-8654, Japan,
[24]Institute for the Advanced Study of Human Biology (ASHBi), Kyoto University, Kyoto 606-8501, Japan,
[25]NEXT-Ganken Program, Japanese Foundation for Cancer Research (JFCR), Tokyo 135-8550, Japan,
[26]Science Groove Inc., Fukuoka 810-0041, Japan,
[27]Department of Virology III, National Institute of Infectious Diseases, Tokyo 208-0011, Japan,
[28]Nuffield Department of Medicine, University of Oxford, Oxford OX3 7FZ, UK.
[29]Research Center for Drug and Vaccine Development, National Institute of Infectious Diseases, Tokyo 162-8640, Japan

¶These authors contributed equally to this work

Transparent Methods

Cell culture. VeroE6/TMPRSS2 cells [VeroE6 cells overexpressing transmembrane protease, serine 2 (TMPRSS2) (Matsuyama et al., 2020) were cultured in Dulbecco's modified Eagle's medium (DMEM; Life Technologies) supplemented with 10% fetal bovine serum (FBS; Cell Culture Bioscience), 100 units/mL penicillin, 100 μg/mL streptomycin, 10 mM HEPES (pH 7.4), and 1 mg/mL G418 (Nacalai) at 37˚C in 5% CO_2. During the infection assay, 10% FBS was replaced with 2% FBS and G418 removed. Calu-3 cells were cultured in above medium supplemented with 10% FBS, 100 units/mL penicillin, and 100 μg/mL streptomycin.

Reagents. All the reagents were purchased from Selleck, Enzo Life Sciences, Cayman Chemical, Sigma, MedChemExpress, TCI or kindly donated by pharmaceutical companies (Abbvie, Alps Pharmaceutical, Asahi Kasei Pharma, Astellas Pharma, Bayer, Boehringer Ingelheim, Bristol-Myers Squibb, Chugai Pharmaceutical, Daiichi Sankyo, EA Pharma, Fujifilm Toyama Chemical, Japan Tobacco, Kakenshoyaku, Kissei Pharmaceutical, Kowa, Kyorin Pharmaceutical, Kyowa Pharmaceutical Industry, Maruho, Mitsubishi Tanabe Pharma, Mochida Pharmaceutical, Novartis, Sanofi, SBI Pharmaceuticals, Shionogi, Sumitomo Dainippon Pharma, Sun Pharma, Takeda Pharmaceutical, Teva Takeda Pharma). Note that throughout in this study we used the pharmaceutical preparation of Cepharanthine (kindly provided by Medisa Shinyaku Inc, a subsidiary of Sawai Pharmaceutical), which is a Stephania-derived alkaloid extract containing 19.5-33.5% Cepharanthine molecule as the major component.

Infection assay. SARS-CoV-2 was handled in a biosafety level 3 (BSL3). We used the SARS-CoV-2 Wk-521 strain, a clinical strain isolated from a COVID-19 patient, and obtained viral stocks by infecting VeroE6/TMPRSS2 cells (Matsuyama et al., 2020). Virus infectious titers were measured by inoculating cells with a 10-fold serial dilution of virus and cytopathology measured to calculate $TCID_{50}$/ml (Matsuyama et al., 2020). For the infection assay, VeroE6/TMPRSS2 cells were inoculated with virus at an MOI of 0.01 (Fig. 1, 2, and 3B, except for 0.001 in Fig. 1B) for 1 h and unbound virus removed by washing. In Fig. 4B, 6, and S1, we used 0.001 of MOI to avoid possible saturation of virus binding/replication. Cells were cultured for 24 h prior to measuring extracellular viral RNA or detecting viral encoded N protein, and cytopathic effects (CPE) after 48 h. Compounds were added during virus inoculation (1 h) and replenished after washing (24 or 48 h) except for time of addition assay. Infection assay with Calu-3 cells was performed by incubation with virus at an MOI of 0.04 for 3 h. N protein was detected at 72 h post-inoculation.

For the time of addition assay, we added compounds with three different timings (Fig. 3A): (a) present during the 1 h virus inoculation step and maintained throughout the 24 h infection period (**whole life cycle**); (b) present during the 1 h virus inoculation step and for an additional 2 h and then removed (**entry**); or (c) added after the inoculation step and present for the remaining 22 h of infection (**post-entry**). Inhibitors of viral replication are expected to show antiviral activity in (a) and (c), but not (b), while entry inhibitors (e.g. chloroquine) reduce viral RNA in all three conditions (In c, addition of entry

inhibitors after inoculation inhibits re-infection and thus decreases viral RNA) (Wang et al., 2020).

Quantification of viral RNA. We mainly quantified viral RNA to measure the antiviral activity of drugs. Viral RNA was extracted with a QIAamp Viral RNA mini, RNeasy mini kit (QIAGEN), or MagMax Viral/Pathogen II Nucleic Acid Isolation kit (Thermo Fisher Scientific) and quantified by real time RT-PCR analysis with a one-step qRT-PCR kit (THUNDERBIRD Probe One-step qRT-PCR kit, TOYOBO) using 5'- ACAGGTACGTTAATAGTTAATAGCGT-3', 5'- ATATTGCAGCAGTACGCACACA-3', and 5'-FAM-ACACTAGCCATCCTTACTGCGCTTCG-TAMRA-3' (E-set) (Corman et al., 2020) or 5'-AAATTTTGGGGAVVAGGAAC-3', 5'-TGGCAGCTGTGTAGGTCAAC-3', and 5'-FAM-ATGTCGCGCATTGGCATGGA-TMARA-3' (N2-set). Detection limit of SARS-CoV-2 RNA for N2-set was 38.1 cycle as C_t cycle.

Detection of viral N protein. Viral protein expression was detected using a rabbit anti-SARS-CoV N antibody (Mizutani et al., 2004) with AlexaFluor 568 anti-rabbit IgG or anti-rabbit IgG-HRP (Thermo Fisher) by indirect immunofluorescence or immunoblot analyses as previously reported (Ohashi et al., 2018).

Cell viability and virus induced cytopathology. Cell viability (Fig. 2B) was determined by MTT assay as previously reported (Ohashi et al., 2018). Virus-induced cytopathology was observed by microscopy at 48 h post-infection as previously reported (Matsuyama et al., 2020). Quantification of cell number (Fig. 1B) was performed with a high-content imaging system as shown below.

Chemical screening. We screened an FDA/EMA/PMDA-approved chemical library composed of 306 compounds by the following cytopathic effect assay to augment the throughput. Cells were treated with compounds at 8, 16, or 30 μM for 1 h during virus inoculation and for up to 72 h post-inoculation. The cells were then fixed with 4% paraformaldehyde and stained with DAPI to count viable cells using a high-content imaging system (ImageXpress Micro Confocal, Molecular Devices). Compounds that protected cells from virus-induced cytopathology and showed cell survival more than 20-fold of the control were selected as hits. Among 306 tested compounds, Cepharanthine, Lopinavir, Loteprednol, Nelfinavir, and Rapamycin were identified as hits. Lopinavir is currently being evaluated in clinical trials for treatment of COVID-19 (Cao et al., 2020). As Loteprednol and Rapamycin are steroid and immunosuppressant, respectively, which suppress immune response, we focused on Cepharanthine and Nelfinavir in this study.

Virus-cell binding assay. SARS-CoV-2 was preincubated with the indicated compounds at 37˚C for 30 min. The SARS-CoV-2 (MOI=0.001) was exposed to VeroE6/TMPRSS2 cells at 4˚C for varying time (5, 15, 30 and 50 min). After extensive wash, total RNA was extracted from cells and viral RNA was quantified by real time RT-PCR to measure cell-bound virus. In this assay, signal/noise ratio of detected RNA for the control with 30 min incubation (Fig. 4B) was more than 300-fold.

Docking simulation of compound binding with a target protein. The crystal structure of the main protease and spike protein were obtained from Protein Data Bank (6LU7 (Jin et al., 2020) and 6M0J (Lan et al., 2020)) and refined for docking simulations using the Protein Preparation Wizard Script within Maestro (Schrödinger, LLC). We carried out *in silico* library screening based on the active site pocket of the main protease using combined molecular docking with a protein-ligand interaction fingerprint scoring method against 8,085 known drugs obtained from the KEGG-Drug database (Kanehisa and Goto, 2000). For all compounds ionization and energy minimization were performed by the OPLS3 force field in the LigPrep Script of Maestro (Schrödinger, LLC). These minimized structures were used as input structures for docking simulations. Docking simulations were performed using the Glide (Friesner et al., 2004; Halgren et al., 2004) SP docking program (Schrödinger, LLC) with a grid box defined by N3 inhibitor molecule for main protease and ACE2 binding interface residues for spike protein using BioLuminate (Schrödinger, LLC)

In vitro SARS-CoV-2 protease assay. The SARS-CoV-2 encoded main protease was purchased from BPS Bioscience, Inc. (USA). The synthesized fluorogenic peptide Ac-Abu-Tle-Leu-Gln-MCA (Rut et al., 2020) was kindly provided by Peptide Institute, Inc. (Japan), and was used as a substrate for the proteolytic assay using the SARS-CoV-2 main protease. The assay was performed in the buffer (20 mM Tri-HCl, pH7.3, 100 mM NaCl, 1 mM DTT, 1 mM EDTA) containing 20 μM of the fluorogenic peptide and 200 nM of the protease. The protease and NFV were pre-incubated at 37°C for 30 min. The reaction was initiated by addition of the substrate and incubated for 30 min at 37°C. The fluorescence of Aminomethylcoumarin due to cleavage of the fluorogenic peptide was monitored at 460 nm with excitation at 380 nm on a fluorescence plate reader (En Spire, Perkin Elmer).

Mathematical analysis. Determination of synergism between NFV and CEP and simulation of virus dynamics as well as the calculation of IIP are shown in detail in Supporting Note.

Statistics. Statistical significance estimated using the two-tailed Student's t test (*$p<0.05$; **$p<0.01$; N.S., not significant).

Supplemental Note, related to Figure 2, 6, and 7.

Quantifying instantaneous inhibitory potential (IIP) from the dose-response curves of the drugs

The typical dose-response curves of a single antiviral drug can be analyzed using the following Hill function (Koizumi et al., 2017) (**Fig. 2A**):

$$f_u = \frac{1}{1 + \left(\frac{D}{IC_{50}}\right)^m}. \qquad (1)$$

Here, f_u represents the fraction of infection events unaffected by the drug (i.e., $1 - f_u$ equals the fraction of drug-affected events). D is the drug concentration, IC_{50} is the drug concentration that achieves 50% inhibition of activity, and m is the slope of the dose-response curve (i.e., Hill coefficient) (Koizumi et al., 2017). Dose-response curves for drugs with higher m values show stronger antiviral activity at the same normalized drug concentration so long as the drug concentration is higher than IC_{50} (**Fig. 2A**). Least-square regression approach was used to fit Eq.(1) to dose-response data and estimate the values of IC_{50} and m. Those estimated values for each drug against SARS-CoV-2 are summarized in **Table S1**.

Expected anti-SARS-CoV-2 effect of double-drug combinations by Bliss independence

We evaluated the effect of double-drug combinations for Bliss independence which is widely used to analyze drug combination data (Bliss, 1939; Kobayashi et al., 2014; Koizumi and Iwami, 2014; Tallarida, 2001). Bliss independence model assumes that each drug acts on different targets/mechanisms, and is defined as:

$$f_u^{\mathrm{Bcom}} = f_u^A(D) \times f_u^B(D), \qquad (3)$$

where f_u^{Bcom}, f_u^A and f_u^B are the fractions of infection events unaffected by the combined drugs A (i.e., Nelfinavir: NFV) and B (i.e., Cepharanthine: CEP) expected by the Bliss model, single drug A and single drug B defined by Eq. (1), respectively. Using Eq. (2), we expected the anti-SARS-CoV2 effects of combined drugs A and B, $1 - f_u^{\mathrm{Bcom}}$, from the anti-SARS-CoV-2 effects of the single drugs (**Fig. S2**).

However, the Bliss model ignores interactions in which drugs enhance each other effects. To address this point, we introduced the recent proposed model (Zimmer et al., 2016), called “dose model” considering the drug interactions, and further evaluated the expected antiviral effects (**Fig. S2**). This drug interaction is described by introducing interaction terms between drug pairs, that is, the “effective” concentration of drug A (i.e., NFV) and B (i.e., CEP), D_A^{com} and D_B^{com}, are defined as follows;

$$D_A^{\mathrm{com}} = D_A\left(1 + a_{AB}\frac{D_B^{\mathrm{com}}}{IC_{50}^B + D_B^{\mathrm{com}}}\right)^{-1}, \qquad D_B^{\mathrm{com}} = D_B\left(1 + a_{BA}\frac{D_A^{\mathrm{com}}}{IC_{50}^A + D_A^{\mathrm{com}}}\right)^{-1},$$

where D_A and D_B are the “true” concentrations, IC_{50}^A and IC_{50}^B are the concentrations that achieve 50% inhibition of activity, a_{AB} and a_{BA} are the interaction parameters for drug A and B, respectively. Note that IC_{50}^A and IC_{50}^B are corresponding to the estimations from the dose-response curves of a

single antiviral drug in combination treatment experiment, which is summarized in **Table S1**, and $a_{AB} = -0.462$ and $a_{BA} = 0.307$ are estimated from the dose-response curves of the double-drug combination. The dose model extended the Bliss model, thus, the expected anti-SARS-CoV-2 effect with effective concentration of drugs A and B (rather than the true concentrations) are calculated as $1 - f_u^{\mathrm{Dcom}}(D)$ and

$$f_u^{\mathrm{Dcom}} = f_u^A(D_A^{\mathrm{com}}) \times f_u^B(D_B^{\mathrm{com}}). \quad (4)$$

The dose model assumed that the effects of drugs on each other's effective doses are multiplicative.

PK/PD/VD model for single- and double-drug combinations against SARS-CoV-2 infection

Based on a standard viral dynamics (VD) model (Ikeda et al., 2016), to describe COVID-19 dissemination among susceptible target cells, we used the following simple mathematical model proposed in (Kim et al., 2020):

$$\frac{df(t)}{dt} = -\beta f(t)V(t), \quad (5)$$

$$\frac{dV(t)}{dt} = \gamma f(t)V(t) - \delta V(t), \quad (6)$$

where $f(t)$ and $V(t)$ are the ratio of uninfected target cells and the amount of virus, respectively. The parameters β, γ, and δ represent the rate constant for virus infection, the maximum rate constant for viral replication and the death rate of infected cells, respectively. All viral load data including Singapore and Zhuhai patients (Young et al., 2020; Zou et al., 2020) were simultaneously fitted using a nonlinear mixed-effect modelling approach, which uses the whole samples to estimate population parameters while accounting for inter-individual variation. The estimated parameters and initial values used here are summarized in **Table S3**.

To investigate the expected outcome for anti-SARS-CoV-2 therapies with single-drug, we conducted *in silico* experiments with the following PK/PD/VD model for replication inhibitor such as Nelfinavir (**Fig. 7**);

$$\frac{df(t)}{dt} = -\beta f(t)V(t), \quad (7)$$

$$\frac{dV(t)}{dt} = \big(1 - \varepsilon(t) \times H(t)\big)\gamma f(t)V(t) - \delta V(t), \quad (8)$$

and for entry inhibitor such as Cepharanthine;

$$\frac{df(t)}{dt} = -\big(1 - \eta(t) \times H(t)\big)\beta f(t)V(t), \quad (9)$$

$$\frac{dV(t)}{dt} = \big(1 - \eta(t) \times H(t)\big)\gamma f(t)V(t) - \delta V(t). \quad (10)$$

Here $H(t)$ is a Heaviside step function defined as $H(t) = 0$ if $t < T$: otherwise $H(t) = 1$, where T is the initiation timing of the treatment, and the anti-SARS-CoV2 effect for $t > T$ are described as

$$\varepsilon(t)\ (\text{or } \eta(t)) = 1 - f_u\big(D(t)\big) = 1 - \frac{1}{1 + \left(\frac{D(t)}{IC_{50}}\right)^m}, \qquad D(t) = C_{max}e^{-kt}$$

where C_{max} and k are the peak drug concentration and the elimination rate for corresponding drug, respectively. The parameter values for each drug used here are summarized in **Table S1 and S2**. Antiviral activities of CEP and NFV were calculated with the expected pharmacokinetics in human lung, based on the pharmacokinetics information for human peripheral blood and that for rat lung and peripheral blood for normalization (Yokoshima et al., 1986; Shetty et al., 1996; Ford et al., 2004).

For anti-SARS-CoV-2 therapies with double-drug combinations, we extended as the following PK/PD/VD model assuming the dose model;

$$\frac{df(t)}{dt} = -\big(1-\eta(t)\times H(t)\big)\beta f(t)V(t), \quad (11)$$

$$\frac{dV(t)}{dt} = \big(1-\varepsilon(t)\times H(t)\big)\big(1-\eta(t)\times H(t)\big)\gamma f(t)V(t) - \delta V(t). \quad (12)$$

Here $H(t)$ is a Heaviside step function defined as $H(t)=0$ if $t<T$: otherwise $H(t)=1$, and the anti-SARS-CoV2 effect are described as

$$\varepsilon(t) = 1 - f_u^A(D_A^{\mathrm{com}}(t)\,) = 1 - \frac{1}{1+\left(\frac{D_A^{\mathrm{com}}(t)}{IC_{50}^A}\right)^{m_A}},$$

$$\eta(t) = 1 - f_u^B\big(D_B^{\mathrm{com}}(t)\big) = 1 - \frac{1}{1+\left(\frac{D_B^{\mathrm{com}}(t)}{IC_{50}^B}\right)^{m_B}},$$

$$D_A^{\mathrm{com}}(t) = C_{\max}^A e^{-k_A t}\left(1 + a_{AB}\frac{D_B^{\mathrm{com}}(t)}{IC_{50}^B + D_B^{\mathrm{com}}(t)}\right)^{-1},$$

$$D_B^{\mathrm{com}}(t) = C_{\max}^B e^{-k_B t}\left(1 + a_{BA}\frac{D_A^{\mathrm{com}}(t)}{IC_{50}^A + D_A^{\mathrm{com}}(t)}\right)^{-1}.$$

Note that we here evaluated the double-drug combination of NFV and CEP (**Fig. 7**), and the pharmacokinetics of NFV and CEP, $D_A^{\mathrm{com}}(t)$ and $D_B^{\mathrm{com}}(t)$, under the combination, are different from those, $D_A(t)$ and $D_B(t)$, under the single-drug treatment because of the effective drug concentration.

Evaluation of outcomes for anti-SARS-CoV-2 therapies

The antiviral effect of the anti-viral therapy on SARS-CoV-2 dynamics using Eqs. (7-12) and our estimated parameter values was calculated (**Fig. 7**). We evaluated the outcomes for the therapies defined as “period until virus elimination” and “reduction of cumulative virus production” (**Fig. S3**). Note that the cumulative virus production, i.e., the area under the curve of viral load (AUC: $\int_0^{T_D} V(s)ds$), for SARS-CoV-2 was calculated, where T_D is the time for SARS-CoV-2 achieved the detection limit.

Supplemental Figure

Fig. S1.

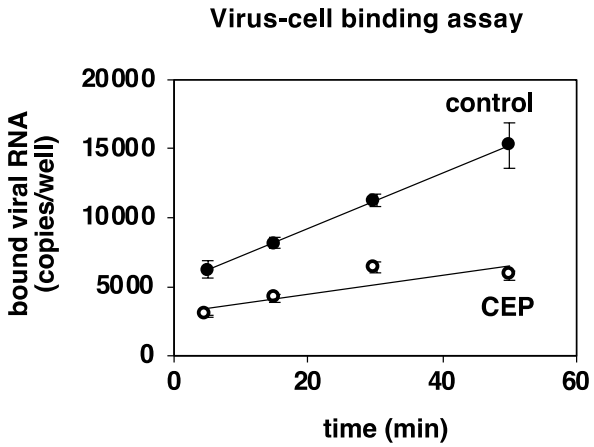

Fig. S1. SARS-CoV-2 binding to cells was inhibited under CEP treatment, related to Figure 4. SARS-CoV-2 pretreated with DMSO (control) or CEP was exposed to VeroE6/TMPRSS2 cells at an MOI of 0.001 in the presence of DMSO (control) or CEP for 5, 15, 30, and 50 min at 4˚C to allow virus-cell binding but not the following steps. After extensive wash, viral RNA was extracted from cells and was quantified by real time RT-PCR analysis. Viral RNA levels bound to cells were linearly increased along with the incubation time and CEP reduced the cell-bound viral RNA at any time points examined. This data was from three independent experiments (mean ± SD).

Fig. S2.

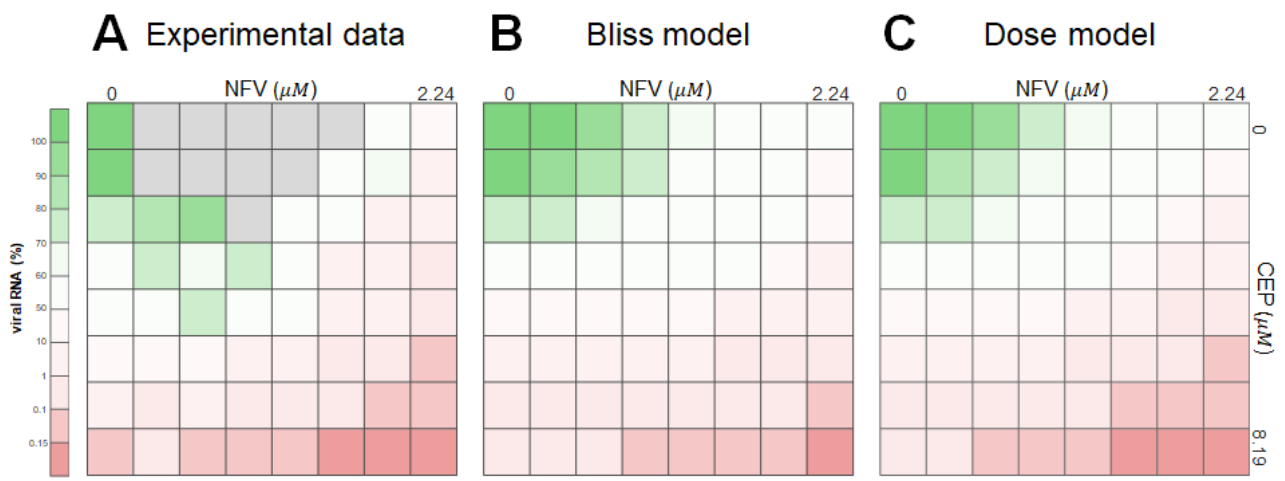

Fig. S2. Comparison of experimental data, Bliss model and Dose model for the double-drug combinations, related to Figure 6. Dose-response matrix of the double-drug combination (corresponding to **Fig. 6A**) are plotted in **(A)**, and the expected anti-SARS-CoV-2 effects of the double-drug combination (NFV and CEP) by the Bliss model and Dose model are plotted in **(B)** and **(C)**, respectively. Note that experimental measurements over 100% of viral RNA (implying large experimental variation because of small dose of antiviral drugs), colored by gray, were excluded in our analysis. The ratios of the values shown in **(A)** over those in **(B)** were calculated and are depicted in **Fig. 6C** in a 3D landscape. To increase the accuracy of evaluation, we employed 1.2-fold serial dilution of NFV from 2.24 μM and 1.6-fold serial dilution of CEP from 8.19 μM.

Fig. S3.

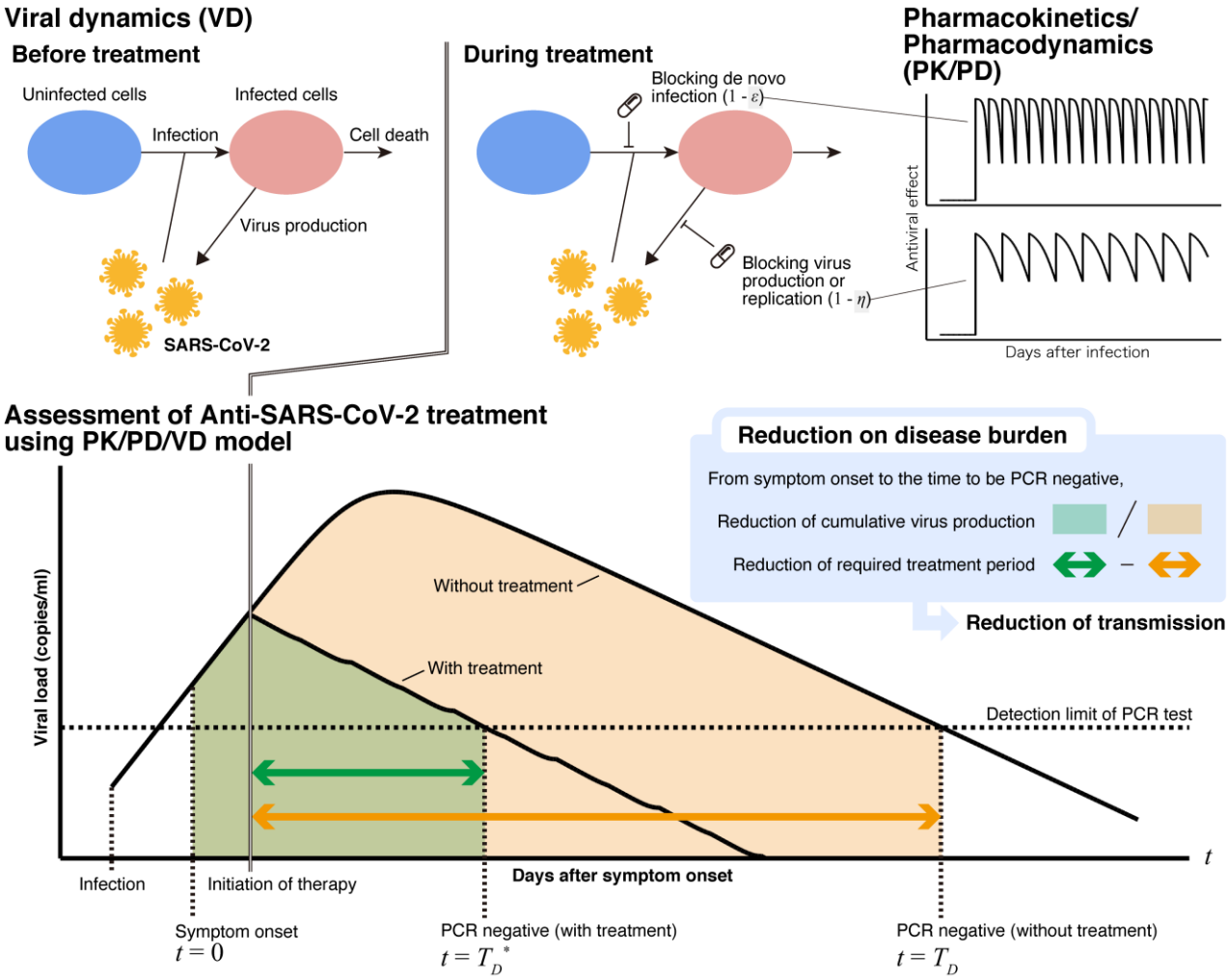

Fig. S3. Schematic representation of SARS-CoV-2 infection dynamics, related to Figure 7. A typical disease progress with viral load on patients undergoing therapy are shown. The outcomes for the therapies, that is, reduction in “period until virus elimination” and “cumulative virus production” are graphically depicted.

Supplemental Tables

Table S1. Estimated characteristic parameters of the tested antiviral drugs, related to Figure 2.

Drug (unit)	Class	IC_{50}	m
Single-drug treatment			
Lopinavir (μM)	RI	3.609	3.852
Nelfinavir (μM)	RI	0.765	5.079
Favipiravir (μM)	RI	4.057×10^{161}	5.610×10^{-3}
Remdesivir (μM)	RI	1.577	3.048
Chloroquine (μM)	EI	1.313	1.984
Cepharanthine (μM)	EI	0.351	2.307
Combination treatment			
Nelfinavir (μM)	RI	1.317	4.043
Cepharanthine (μM)	EI	0.991	3.174

RI, replication inhibitor; EI, entry inhibitor

IC_{50}, 50% inhibitory concentration

m, slope of the dose-response curve (i.e., Hill coefficient)

Table S2. Summary of pharmacokinetic parameters of anti-SARS-CoV-2 drugs, related to Figure 7.

Parameter name	Symbol	Unit	Nelfinavir*	Cepharanthine**	
				i.v.	p.o.
Single-compartment model					
Maximum concentration	C_{max}	μM	9.32	12.3	3.49×10^{-2}
Degradation rate	k	day^{-1}	4.89	0.318	
Dosing schedule					
Initiation of treatment	t^*	day		0.500	
Dosing interval	τ	day	0.333	7.00	1.00

Nelfinavir: 500 mg, TID, orally

Cepharanthine: 25mg, intravenous drip (i.v.) or 10 mg, oral administration (p.o.)

* Expected pharmacokinetics information in human lung. We estimated the scaling parameter of C_{max} between lung and peripheral blood in rats (Shetty et al., 1996). We then calculated C_{max} in human lung based on that in human peripheral blood assuming the scaling parameter is the same between humans and rats. Since the half-life of NFV in the cells was reported to be almost the same as that in plasma (Ford et al., 2004), we used the information for the half-life of NFV in plasma for that in the lung.

** Expected pharmacokinetics information in human lung. We estimated the degradation rate, k, in rat lung (Yokoshima et al., 1986), and the scaling parameter of C_{max} between lung and peripheral blood in rat. Then we used the degradation rate for human lung and calculated C_{max} in human lung by that in human peripheral blood assuming the scaling parameter is same between humans and rats.

Table S3. Estimated population parameters and initial values for SARS-CoV-2 infection, related to Figure 7.

Parameter name	Symbol	Unit	Value
Maximum rate constant for viral replication	γ	day^{-1}	3.16
Rate constant for virus infection	β	$(copies/ml)^{-1}\ day^{-1}$	9.77×10^{-6}
Death rate of infected cells	δ	day^{-1}	0.615
Initial viral load	$V(0)$	copies/ml	5.64×10^{3}

Supplemental References

Bliss, C. (1939). The toxicity of poisons applied jointly1. Annals of applied biology. 26(3), 585-615.

Cao, B., Wang, Y., Wen, D., Liu, W., Wang, J., Fan, G., Ruan, L., Song, B., Cai, Y., Wei, M., et al. (2020). A Trial of Lopinavir-Ritonavir in Adults Hospitalized with Severe Covid-19. N Engl J Med. Published online 2020/03/19 DOI: 10.1056/NEJMoa2001282.

Corman, V.M., Landt, O., Kaiser, M., Molenkamp, R., Meijer, A., Chu, D.K.W., Bleicker, T., Brunink, S., Schneider, J., Schmidt, M.L., et al. (2020). Detection of 2019 novel coronavirus (2019-nCoV) by real-time RT-PCR. Euro Surveill. 25(3). Published online 2020/01/30 DOI: 10.2807/1560-7917.ES.2020.25.3.2000045.

Friesner, R.A., Banks, J.L., Murphy, R.B., Halgren, T.A., Klicic, J.J., Mainz, D.T., Repasky, M.P., Knoll, E.H., Shelley, M., Perry, J.K., et al. (2004). Glide: a new approach for rapid, accurate docking and scoring. 1. Method and assessment of docking accuracy. J Med Chem. 47(7), 1739-1749. Published online 2004/03/19 DOI: 10.1021/jm0306430.

Halgren, T.A., Murphy, R.B., Friesner, R.A., Beard, H.S., Frye, L.L., Pollard, W.T., and Banks, J.L. (2004). Glide: a new approach for rapid, accurate docking and scoring. 2. Enrichment factors in database screening. J Med Chem. 47(7), 1750-1759. Published online 2004/03/19 DOI: 10.1021/jm030644s.

Ikeda, H., Nakaoka, S., de Boer, R.J., Morita, S., Misawa, N., Koyanagi, Y., Aihara, K., Sato, K., and Iwami, S. (2016). Quantifying the effect of Vpu on the promotion of HIV-1 replication in the humanized mouse model. Retrovirology. 13, 23. Published online 2016/04/19 DOI: 10.1186/s12977-016-0252-2.

Jin, Z., Du, X., Xu, Y., Deng, Y., Liu, M., Zhao, Y., Zhang, B., Li, X., Zhang, L., Peng, C., et al. (2020). Structure of M(pro) from COVID-19 virus and discovery of its inhibitors. Nature. Published online 2020/04/10 DOI: 10.1038/s41586-020-2223-y.

Kanehisa, M., and Goto, S. (2000). KEGG: kyoto encyclopedia of genes and genomes. Nucleic Acids Res. 28(1), 27-30. Published online 1999/12/11 DOI: 10.1093/nar/28.1.27.

Kim, K.S., Ejima, K., Ito, Y., Iwanami, S., Ohashi, H., Koizumi, Y., Asai, Y., Nakaoka, S., Watashi, K., Thompson, R.N., et al. (2020). Modelling SARS-CoV-2 Dynamics: Implications for Therapy. medRxiv. 2020.2003.2023.20040493. DOI: 10.1101/2020.03.23.20040493.

Kobayashi, T., Koizumi, Y., Takeuchi, J.S., Misawa, N., Kimura, Y., Morita, S., Aihara, K., Koyanagi, Y., Iwami, S., and Sato, K. (2014). Quantification of deaminase activity-dependent and -independent restriction of HIV-1 replication mediated by APOBEC3F and APOBEC3G through experimental-mathematical investigation. J Virol. 88(10), 5881-5887. Published online 2014/03/14 DOI: 10.1128/jvi.00062-14.

Koizumi, Y., and Iwami, S. (2014). Mathematical modeling of multi-drugs therapy: a challenge for determining the optimal combinations of antiviral drugs. Theor Biol Med Model. 11, 41. Published online 2014/09/26 DOI: 10.1186/1742-4682-11-41.

Koizumi, Y., Ohashi, H., Nakajima, S., Tanaka, Y., Wakita, T., Perelson, A.S., Iwami, S., and Watashi, K. (2017). Quantifying antiviral activity optimizes drug combinations against hepatitis C virus infection. Proc Natl Acad Sci U S A. 114(8), 1922-1927. Published online 2017/02/09 DOI: 10.1073/pnas.1610197114.

Lan, J., Ge, J., Yu, J., Shan, S., Zhou, H., Fan, S., Zhang, Q., Shi, X., Wang, Q., Zhang, L., et al. (2020). Structure of the SARS-CoV-2 spike receptor-binding domain bound to the ACE2 receptor. Nature. Published online 2020/04/01 DOI: 10.1038/s41586-020-2180-5.

Matsuyama, S., Nao, N., Shirato, K., Kawase, M., Saito, S., Takayama, I., Nagata, N., Sekizuka, T., Katoh, H., Kato, F., et al. (2020). Enhanced isolation of SARS-CoV-2 by TMPRSS2-expressing cells. Proc Natl Acad Sci U S A. 117(13), 7001-7003. Published online 2020/03/14 DOI: 10.1073/pnas.2002589117.

Mizutani, T., Fukushi, S., Saijo, M., Kurane, I., and Morikawa, S. (2004). Phosphorylation of p38 MAPK and its downstream targets in SARS coronavirus-infected cells. Biochem Biophys Res Commun. 319(4), 1228-1234. Published online 2004/06/15 DOI: 10.1016/j.bbrc.2004.05.107.

Ohashi, H., Nishioka, K., Nakajima, S., Kim, S., Suzuki, R., Aizaki, H., Fukasawa, M., Kamisuki, S., Sugawara, F., Ohtani, N., et al. (2018). The aryl hydrocarbon receptor-cytochrome P450 1A1 pathway controls lipid accumulation and enhances the permissiveness for hepatitis C virus assembly. J Biol Chem. 293(51), 19559-19571. Published online 2018/11/02 DOI: 10.1074/jbc.RA118.005033.

Rut, W., Groborz, K., Zhang, L., Sun, X., Zmudzinski, M., Hilgenfeld, R., and Drag, M. (2020). Substrate specificity profiling of SARS-CoV-2 Mpro protease provides basis for anti-COVID-19 drug design. https://doi.org/10.1101/2020.03.07.981928.

Tallarida, R.J. (2001). Drug synergism: its detection and applications. J Pharmacol Exp Ther. 298(3), 865-872. Published online 2001/08/16.

Wang, M., Cao, R., Zhang, L., Yang, X., Liu, J., Xu, M., Shi, Z., Hu, Z., Zhong, W., and Xiao, G. (2020). Remdesivir and chloroquine effectively inhibit the recently emerged novel coronavirus (2019-nCoV) in vitro. Cell Res. 30(3), 269-271. Published online 2020/02/06 DOI: 10.1038/s41422-020-0282-0.

Yabuki, T., Motoda, Y., Hanada, K., Nunokawa, E., Saito, M., Seki, E., Inoue, M., Kigawa, T., and Yokoyama, S. (2007). A robust two-step PCR method of template DNA production for high-throughput cell-free protein synthesis. J Struct Funct Genomics. 8(4), 173-191. Published online 2008/01/02 DOI: 10.1007/s10969-007-9038-z.

Yokoshima, T., Tsutsumi, S., Ohtsuki, T., Takaichi, M., Nakajima, T., and Akasu, M. (1986). Studies on metabolic fate of cepharanthine: Absorption, distribution, metabolism and excretion in rats. Pharmaceutical Regulatory Science. 17(3), 458-479.

Young, B.E., Ong, S.W.X., Kalimuddin, S., Low, J.G., Tan, S.Y., Loh, J., Ng, O.T., Marimuthu, K., Ang, L.W., Mak, T.M., et al. (2020). Epidemiologic Features and Clinical Course of Patients Infected With SARS-CoV-2 in Singapore. Jama. Published online 2020/03/04 DOI: 10.1001/jama.2020.3204.

Zimmer, A., Katzir, I., Dekel, E., Mayo, A.E., and Alon, U. (2016). Prediction of multidimensional drug dose responses based on measurements of drug pairs. Proc Natl Acad Sci U S A. 113(37), 10442-10447. Published online 2016/08/27 DOI: 10.1073/pnas.1606301113.

Zou, L., Ruan, F., Huang, M., Liang, L., Huang, H., Hong, Z., Yu, J., Kang, M., Song, Y., Xia, J., et al. (2020). SARS-CoV-2 Viral Load in Upper Respiratory Specimens of Infected Patients. N Engl J Med. Published online 2020/02/20 DOI: 10.1056/NEJMc2001737.